

51-18
12 111
N96-16685

Sensitivity of Planetary Cruise Navigation to Earth Orientation Calibration Errors

J. A. Estefan

Navigation and Flight Mechanics Section

W. M. Folkner

Tracking Systems and Applications Section

A detailed analysis was conducted to determine the sensitivity of spacecraft navigation errors to the accuracy and timeliness of Earth orientation calibrations. Analyses based on simulated X-band (8.4-GHz) Doppler and ranging measurements acquired during the interplanetary cruise segment of the Mars Pathfinder heliocentric trajectory were completed for the nominal trajectory design and for an alternative trajectory with a longer transit time. Several error models were developed to characterize the effect of Earth orientation on navigational accuracy based on current and anticipated Deep Space Network calibration strategies. The navigational sensitivity of Mars Pathfinder to calibration errors in Earth orientation was computed for each candidate calibration strategy with the Earth orientation parameters included as estimated parameters in the navigation solution. In these cases, the calibration errors contributed 23 to 58 percent of the total navigation error budget, depending on the calibration strategy being assessed. Navigation sensitivity calculations were also performed for cases in which Earth orientation calibration errors were not adjusted in the navigation solution. In these cases, Earth orientation calibration errors contributed from 26 to as much as 227 percent of the total navigation error budget. The final analysis suggests that, not only is the method used to calibrate Earth orientation vitally important for precision navigation of Mars Pathfinder, but perhaps equally important is the method for inclusion of the calibration errors in the navigation solutions.

I. Introduction

Radio metric data, particularly two-way coherent Doppler and range, have been used to navigate robotic spacecraft since the inception of planetary exploration. For a spacecraft in interplanetary cruise or transit, much of the information content inherent in the data for position determination comes from the signature imposed on the station-spacecraft radio signal by the Earth's rotation [1-3]. The diurnal signature in the radio metric data yields information about the right ascension and declination of the spacecraft with respect to the direction of the Earth's spin axis at the time of observation. The orientation of the Earth, as a function of time, must be known with respect to inertial space in order to effectively utilize the radio metric data to deduce spacecraft position with respect to the target planet. Errors in Earth orientation thus lead to targeting errors for spacecraft approaching other planetary bodies.

Evidence of the need to adequately account for Earth orientation errors came as early as April 1965 when flight project navigation teams for the Rangers VII and VIII lunar probes observed a large difference in station longitude solutions for all deep-space stations using radio metric data [4]. This was later determined to be the result of improper Earth orientation calibration. As a result, Earth orientation calibration methods were later refined to support the Mariners IV and V planetary exploration missions.

To assess the effect of Earth orientation calibration errors on interplanetary cruise navigation for both current and future Deep Space Network (DSN) Earth orientation calibration techniques, a navigation error analysis of the Mars Pathfinder approach scenario was performed. Mars Pathfinder has the most stringent planetary cruise navigation requirements of any currently planned mission. Other Mars lander missions similar to Pathfinder are being studied. Navigation performance for these future missions may exhibit different sensitivity characteristics to Earth orientation calibration errors since the sensitivity is trajectory dependent. In this study, two Mars approach trajectories were evaluated, the nominal Pathfinder cruise trajectory with arrival at Mars on July 4, 1997, and a second trajectory with a longer transit time. Clearly, restricting the study to only two trajectories is far from encompassing the entire range of possible planetary approach scenarios. Moreover, actual navigation performance will vary depending on targeting point and targeting requirements, the data type and arc length, filtering strategy, and observation geometry, which could vary depending on each launch opportunity (especially spacecraft right ascension and declination at encounter). The study of two "representative" trajectories, while limited, at least provides some insight into the possible range of navigational uncertainties caused by Earth orientation calibration errors.

Other types of navigation problems have varying sensitivity to Earth orientation error. For spacecraft in close orbit about another planetary body, such as Magellan or Mars Global Surveyor (MGS), the primary signature on the spacecraft radio signal is imposed by the orbit about the planet. Doppler measurements can be used to determine all spacecraft orbital elements in most cases, and the resultant orbit determination is largely insensitive to Earth orientation errors. If, however, the orbit determination using Doppler data is not accurate enough to meet the mission requirements, two-station differenced-Doppler or narrow-band very long baseline interferometry (VLBI) observations can be used for improved orbit determination in some cases. In fact, the Magellan project utilized differenced-Doppler data for this purpose. A detailed sensitivity analysis of differenced-Doppler navigation to Earth orientation calibration errors is not presented in this article, but a cursory approximation is given in Appendix A. In contrast to spacecraft in close planetary orbit, the Galileo and Cassini spacecraft will be in long-period (~ 120 -day) orbits about Jupiter and Saturn, respectively. These represent an intermediate case between planetary approach and low planetary orbit, so some sensitivity to Earth orientation errors might be expected. Onboard optical images of planetary satellites will be an important data type in determining the orbits for Galileo and Cassini. The added complexity of blending onboard optical data with radio metric data precluded this study from assessing the navigation sensitivity to Earth orientation errors for these outer planet orbiters.

In this article, a navigation error analysis is described that was used to assess the impact of various Earth orientation calibration strategies on predicted spacecraft orbit determination accuracies during interplanetary cruise. Section II provides the fundamental framework for defining the principal parameters that are used to characterize Earth orientation, while Section III focuses on the Earth orientation calibration process used by the DSN. These discussions are followed by a description in Section IV of the origin and format of the functional requirements levied on the DSN tracking system by the flight projects. In Section V, a simple information content analysis is presented to obtain a rough estimate of the influence of Earth orientation errors on Doppler cruise navigation performance. Section VI describes the assumptions used in a linear covariance analysis to evaluate the sensitivity of spacecraft navigational accuracies to Earth orientation calibration errors for two Mars Pathfinder approach scenarios. Various Earth orientation calibration strategies are described, together with tracking data simulation and error modeling assumptions. Results and key observations from the numerical assessment are summarized and discussed at the conclusion of the article.

II. Earth Orientation Parameters

The Earth is an oblate, spinning body that undergoes precession and nutation due to the torques exerted upon it by the Sun, Moon, and other planets. The north pole of a body-fixed (crust-fixed) coordinate system varies unpredictably with respect to the spin direction, due to internal dynamics of the Earth and its atmosphere (a process called “polar motion”). Similar effects cause the Earth’s rotation rate to vary unpredictably. (The variations in the rotation rate are several times larger than the polar motion variations.)

The orientation of a body in inertial space can be completely described by three Euler angles. Because the Earth rotates rapidly, the three angles describing the orientation of the surface with respect to inertial space vary rapidly with time. Conventionally, the orientation of the Earth is described by five angles that vary slowly with time, rather than by three rapidly varying angles. These five angles are described in greater detail below.

In the development of the 1980 International Astronomical Union (IAU) theory of nutation [5], the concept of the celestial ephemeris pole (CEP) was introduced. The CEP was defined such that there are no nearly diurnal motions of the CEP with respect to either space-fixed (inertial) or body-fixed coordinates. For a rigid body with no polar motion, the CEP corresponds to the body axis about which the body is spinning.

The motion of the CEP in space-fixed coordinates, due to precession and nutation, can be described by the two angles, ψ and ε , where ε is the obliquity (inclination of the equatorial plane to the Earth’s orbital plane) and ψ is the intersection of the equator and orbit with respect to a fixed equinox. The variation in the Earth’s rotation about the CEP affects the time at which celestial objects cross the apparent meridian and is measured by a quantity called Universal Time (UT) (specifically, Universal Time 1, or “UT1”). Variations of the CEP in body-fixed coordinates are measured by the quantities polar motion “X” and polar motion “Y”.

Because of the random variation of UT1 and polar motion (along with imperfect modeling of precession and nutation), an accurate description of Earth orientation requires continual monitoring. VLBI data can be used to determine all components of Earth orientation with 5 nrad or better accuracy (1-sigma).¹ Because VLBI measurements require correlation of large volumes of data from ground stations separated by large distances, there is usually a time delay between the acquisition of raw VLBI data and the processing of the data that determines the Earth orientation angles. This processing delay is currently 2 to 3 days for DSN VLBI measurements made for rapid determination of Earth orientation (i.e., TEMPO measurements, described in Section III); the delay is longer for VLBI data from external services. Satellite laser ranging (SLR) or Global Positioning System (GPS) data can also be used to determine polar motion and small changes in UT1 with shorter data-processing times but are not able to directly measure all five Earth orientation angles. Atmospheric angular momentum (AAM) data are highly correlated with variation in UT1 and the length of the day (LOD), a parameter proportional to the rate of change of UT1. Therefore, AAM data, both measurements and forecasts, have been used to improve predictions for both UT1 and LOD [6].

Precession/nutation models with parameters adjusted to fit the observed space-fixed motion of the CEP, e.g., [7,8], have an accuracy of 5 nrad or better over the time of the fit. These models can be used to predict precession and nutation for periods of about 1 year before discrepancies systematically exceed 5 nrad. Figure 1 shows a comparison of the daily correction calibrations (from 1991 to 1995) with a model by Steppe et al. fit to data through the end of 1993 [9]. The nutation corrections are with respect

¹ Earth orientation accuracies are often quoted in a variety of units. An angle of 5 nrad is approximately equal to 1 milliarc-second (mas). An angular rotation of 5 nrad corresponds to a change in position on the surface of the Earth (equatorial displacement) of about 3 cm. A change in UT1 of 1 millisecond (ms) corresponds to an angle of about 15 mas, which is equivalent to an angle of 75 nrad, or to an equatorial displacement of roughly 50 cm.

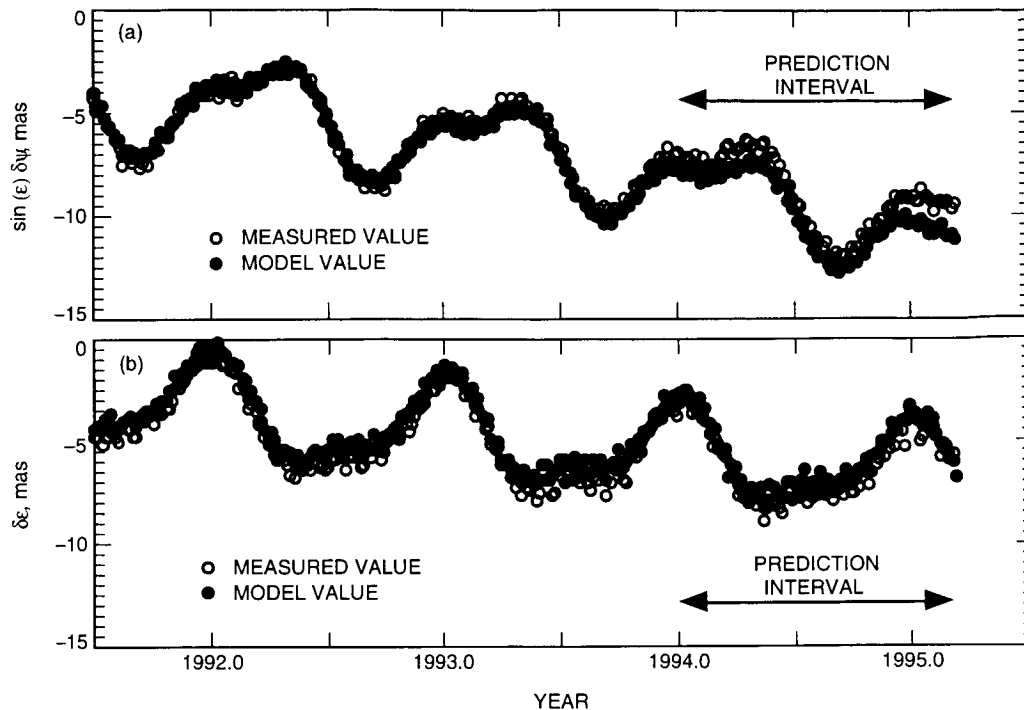


Fig. 1. A comparison of a nutation correction model to observations. The correction angles (a) $\sin(\epsilon) \delta\psi$ and (b) $\delta\epsilon$ are corrections to the IAU (1976) nutation model [5]. (A change of $\delta\epsilon$ or $\sin(\epsilon) \delta\psi$ of 1 mas corresponds to a shift in the inertial position of a point on the Earth's surface of about 3 cm.)

to the 1976 IAU precession model [10,11] and 1980 IAU nutation model [5]. The corrections are currently about 10 mas (~ 50 nrad) and are increasing with time. It can be seen that the predictions of the model fit to data through the end of 1993 agree with the later measurements to an accuracy of about 1 mas for about 1 year.

UT1 and polar motion (collectively referred to as UTPM throughout this article) vary randomly due to the interaction of the atmosphere and the crust. UT1 varies much more rapidly than polar motion. Random variation in UT1 can be characterized by an integrated random walk, while polar motion behaves approximately as an integrated Gauss-Markov process [12]. UT1 varies by an amount corresponding to an angle of 1 mas in about 1 day, so continual, rapid calibration is required to be able to completely describe Earth orientation to 1-mas accuracy.

III. Earth Orientation Calibrations

At the Jet Propulsion Laboratory (JPL), Earth orientation calibrations are currently determined by the DSN's Time and Earth Motion Precision Observations (TEMPO) activity. TEMPO, which became operational in late 1983, was chartered to provide an operational Earth orientation service both to support JPL's spacecraft navigation efforts and to serve the worldwide community [13]. TEMPO supports Earth orientation calibration by performing VLBI measurements at regular intervals (currently twice per week) using the DSN's 70-m antenna subnetwork. (Prior to 1983, Earth orientation calibrations were provided by the DSN's Tracking System Analytic Calibration (TSAC) activity, which produced calibrations based on monthly estimates of UTPM disseminated by the Bureau Internationale de l'Heure (BIH) in Paris, France.)² The Kalman Earth Orientation Filter (KEOF) is used to combine the TEMPO measurements

²T. F. Runge, personal communication, Tracking Systems and Applications Section, Jet Propulsion Laboratory, Pasadena, California, February 1995.

with other sources of Earth orientation information. By performing regular VLBI measurements and including AAM measurements and forecasts, together with other data from Earth orientation services outside JPL, the DSN can deliver, at any time, an Earth orientation calibration accurate to 50 nrad (1-sigma) [6]. Earth orientation accuracy is better for times 15 days or more in the past, for which a greater amount of processed VLBI data from external services is available. Earth orientation predictions are also delivered, with accuracies that degrade with time due to the random behavior of UTPM. Efforts are ongoing to improve these predictions both by modeling improvements within the KEOF and by better utilization of geodetic and AAM data.³

The standard DSN Earth orientation calibration file (referred to as a UTPM STOIC file) is a text file of polynomial coefficients that provides UTPM calibrations for 37 specified times.⁴ Precession and nutation calibrations are not included. The limitation to 37 calibration times has implications for the accuracy of Earth orientation available to the end-user (e.g., navigation teams) because of the integrated-random walk characteristic of UTPM. Several flight projects utilize calibration files that span a year or more, giving 10-day spacing (or more) between calibration times. Midway between respective calibrations at 10-day intervals, the expected (1-sigma) error in UT1 is about 0.4 ms (~20 cm) even if the calibration is perfect at the calibration times. This limitation, together with the lack of precession/nutation calibrations, has led to a new DSN calibration file—the Earth-Orientation Parameter (EOP) file—which includes precession and nutation corrections and has no limit on the number of calibration times.⁵ It should be noted that all timing calibrations and their rates are given with respect to a reference time defined by atomic clocks, specifically, International Atomic Time (TAI).

IV. Functional Requirements

Navigation-related requirements for current and future missions are defined primarily by flight projects and future mission study teams. These requirements serve as a starting point to establish DSN ground support requirements to satisfy mission navigation. In the past, navigation requirements for calibrations such as Earth orientation, station locations, and transmission media typically have been arrived at in an ad hoc manner without thorough analysis. This practice has at times resulted in confusion and later cancellation of implementation plans to develop calibrations for which there was an erroneously believed need.

Arguably, flight projects and future mission study teams find it more economical to simply adopt past calibration performance or to adopt anticipated improvements in the calibrations rather than conduct a parametric study in which all possible navigation calibrations are investigated. In order to meet mission navigation needs, the DSN has documented UTPM calibration capabilities and requirements for the tracking and navigation subsystems.^{6,7} The current UTPM requirements are stated as: “(a) 30 cm (1-

³ J. O. Dickey, personal communication, Tracking Systems and Applications Section, Jet Propulsion Laboratory, Pasadena, California, August 1995.

⁴ In the early 1970s, all UTPM calibration data for mission operations were supplied in a single computer card deck called a PLATO deck (Platform Observables). The PLATO system replaced the former Timing and Polynomial (TPOLY) computer program for generating separate timing calibration data [14]. For contingency purposes, a smaller and simpler backup program was developed to generate PLATO-style decks that could be delivered rapidly in the event PLATO was not operable. This program was called STOIC (Standby Timing Operation In Contingencies)—hence, the frequently encountered convention “STOIC” file or, more appropriately, “UTPM STOIC” file. Sometimes, these files are referred to by their historical convention as “TPOLY” files or simply as “TP” arrays.

⁵ *DSN Tracking System Interfaces, Earth Orientation Parameter Data Interface (TRK-2-21), DSN System Requirements Detailed Interface Design*, JPL 820-13, Rev. A (internal document), Jet Propulsion Laboratory, Pasadena, California, April 19, 1985.

⁶ *DSN System Functional Requirements and Design: Tracking System (1988 Through 1993)*, JPL 821-19, Rev. C (internal document), Jet Propulsion Laboratory, Pasadena, California, pp. 3-20, April 15, 1993.

⁷ *NOCC Subsystem Functional Requirements: Navigation Subsystem (1988 Through 1993)*, JPL 822-18, Rev. A (internal document), Jet Propulsion Laboratory, Pasadena, California, pp. 3-7-3-8, May 15, 1988.

sigma) in each component, predictive, for the days on which the calibrations are generated; (b) 5 cm (1-sigma) in each component, non-predictive, for periods through 14 days prior to the day on which the calibrations are generated; (c) 5 to 25 cm (1-sigma) in each component of polar motion, non-predictive, for periods from 1962 through 1984; and (d) 10 to 40 cm (1-sigma) in UT1, non-predictive, for periods from 1962 through 1984.”⁸

The exact origin of the 30-cm real-time knowledge requirement is not widely known, although it is clear that it was arrived at via the common practice of synthesizing past flight project navigation team requirements and what the current calibration activity claimed could be delivered in terms of accuracy and timeliness. There is a common misconception that the 30-cm functional requirement for all three components of UTPM was driven by Magellan mission requirements. In actuality, the Magellan 30-cm requirement was inherited directly from the Galileo project for a 30-cm real-time UTPM knowledge requirement.⁹ The UTPM requirements levied by future missions (e.g., Cassini, MGS) vary from flight project to flight project and are subject to change. Therefore, mission-specific requirements will not be presented here. It is fair to state that an effort is under way to update the overall Earth orientation calibration functional requirements for Mars Pathfinder (precession/nutation as well as UTPM) based on the analysis presented in this article.

V. Information Content Analysis

Early analytic studies suggest that Earth orientation uncertainties result in equivalent uncertainties in the instantaneous location of tracking stations, which leads to a degradation in the apparent quality of the radio metric data used for navigation [15–17]. As noted in the introductory remarks, timing (UT1) errors in particular can lead to an erroneous prediction of the spacecraft coordinates near planetary encounter. Much of Doppler data’s information content, when acquired during interplanetary cruise, comes from the diurnal signature of the Earth’s rotation. This is evident in a simple analytic representation of the instantaneous range rate, $\dot{\rho}$, observed by an Earth-based tracking station [1–3]:

$$\dot{\rho} = v_r + r_s \omega_e \cos \delta \sin \omega_e t + (-\Delta\alpha + \Delta\lambda + \omega_e \Delta UT1) r_s \omega_e \cos \delta \cos \omega_e t \quad (1)$$

Here, v_r denotes the spacecraft radial velocity with respect to the Earth; r_s is the distance of the station from the Earth’s spin axis, ω_e denotes the rotation rate of the Earth, and t is measured from the nominal time the spacecraft crosses the tracking station’s meridian. The δ is the instantaneous declination of the spacecraft, $\Delta\alpha$ the correction to the a priori value of spacecraft right ascension, $\Delta\lambda$ the correction to the station longitude, and $\Delta UT1$ the correction to rotation about the spin axis. There are, of course, other parameters to be estimated. Moreover, this simple model neglects the additional geometric strength that comes from the motion of the Earth about the Sun and the use of multiple tracking stations. Nevertheless, this model is useful to illustrate (to first order) the effect of Earth orientation errors on the Doppler data.

It is clear from Eq. (1) that an error in rotation about the Earth’s spin axis would directly affect the right ascension estimate. For example, at Deep Space Station (DSS) latitudes (~ 35 deg), a 1-ms timing error is equivalent to a longitude error of about 0.4 m, or a right ascension error of about 0.07 μ rad [13]. Polar motion affects the spacecraft position estimate by producing displacements in the station spin radius, longitude, and height above the equator. These displacements can be as large as 10 m if not properly calibrated. Equation (1) expresses the spacecraft right ascension and declination with respect to the Earth’s equator of date. Errors in precession and nutation models can lead to errors in the transformation of the “of-date” right ascension and declination estimate into the inertial coordinate

⁸ Ibid.

⁹ S. N. Mohan and W. L. Sjogren, “Revised Navigation Requirement Specification for the VRM Mission Requirements Document 630-6 and Preliminary Spacecraft Instrumentation Requirements Document (SIRD),” JPL Interoffice Memorandum 314.10-348, Rev. 1 (internal document), Jet Propulsion Laboratory, Pasadena, California, September 22, 1983.

system of the planetary ephemeris. Precession/nutation modeling errors are rarely significant for Earth-orbiting spacecraft, where the observational data tie the spacecraft orbit much more tightly to a local coordinate system. For interplanetary spacecraft, the trajectory determined by Earth-based radio metric data must be related to the position of a distant planet.

VI. Navigation Error Analysis

To investigate the effect of various levels of Earth orientation calibration accuracy on interplanetary cruise navigation, an error covariance analysis of the Mars Pathfinder approach segment was performed. The Mars Pathfinder approach scenario was selected because it has the most stringent planetary approach navigation requirements of any currently planned mission. Future Mars lander missions may utilize different trajectory designs and potentially could exhibit a lesser or greater level of sensitivity to Earth orientation calibration errors than those presented herein. This analysis is intended to serve as a representative model.

A. Calibration Strategies (Test Cases)

In order to study the effect of Earth orientation calibrations on Mars Pathfinder cruise navigation, six test cases were developed to cover a wide range of possible Earth orientation calibration strategies. The level of calibration errors, which are a function of time, depends on the amount of data included in creation of the calibration files and on the timeliness of their deliveries. Precession/nutation calibrations were not included in this study since it is possible to predict the corrections for about a year with an accuracy approaching ~ 1 mas. All cases of Earth orientation studied here assume a basic set of VLBI measurements that can provide this level of precession/nutation accuracy (cf., Section II).

The Earth orientation calibration cases are characterized by the uncertainty in UT1 and polar motion as a function of time and by the correlations between the errors at different times. The reference day for the Earth orientation calibration cases is the day on which the navigation solution is performed. Figure 2 shows the assumed uncertainty in UT1 for the six cases, while Fig. 3 illustrates the assumed polar motion uncertainties. To simplify the analysis, the indicated level of polar motion uncertainty was assumed for both the X and Y components independently, even though actual measurements show that uncertainty in predictions for polar motion Y increase about 30 percent slower than for polar motion X [12]. Table 1 gives additional information about the statistics of each Earth orientation case. In all cases, the errors due to the potentially sparse array of calibration times imposed by the STOIC file have been neglected since this effect can be removed either by use of the EOP file or by use of a STOIC file that spans the shortest time possible.

The baseline Earth orientation case is the current nominal DSN capability and is indicated as TEMPO in the figures and in Table 1 [6].¹⁰ This is based on two DSN VLBI measurements per week combined with data available from other sources. It is assumed that the last processed TEMPO VLBI measurement of UT1 was acquired 5 days before the KEOF filter run and that the KEOF filter run is performed 1 day prior to the navigation solution. For UT1 prediction, the rate of change in UT1 is important. The UT1 rate is dependent on the last two processed TEMPO measurements. For this particular case, UT1 was characterized as a first-order Gauss-Markov random process with a 1-sigma steady-state uncertainty of 0.11 ms and a 5-day correlation time until 7 days prior to the navigation solution; from this time forward, UT1 uncertainty was characterized by an integrated random walk (through the time of the navigation solution). The current KEOF filter solutions include the TEMPO VLBI measurements and AAM measurements and forecasts to give the stated capability for UT1 accuracy on any given day. In addition, daily VLBI measurements from external services are included in the KEOF filter solutions to provide the steady-state uncertainty of 0.11 ms for times in the past. (The 0.11 ms is larger than the

¹⁰ A. P. Freedman, "Polar Motion Prediction With KEOF," JPL Interoffice Memorandum 335.2-92.01 (internal document), Jet Propulsion Laboratory, Pasadena, California, March 5, 1992.

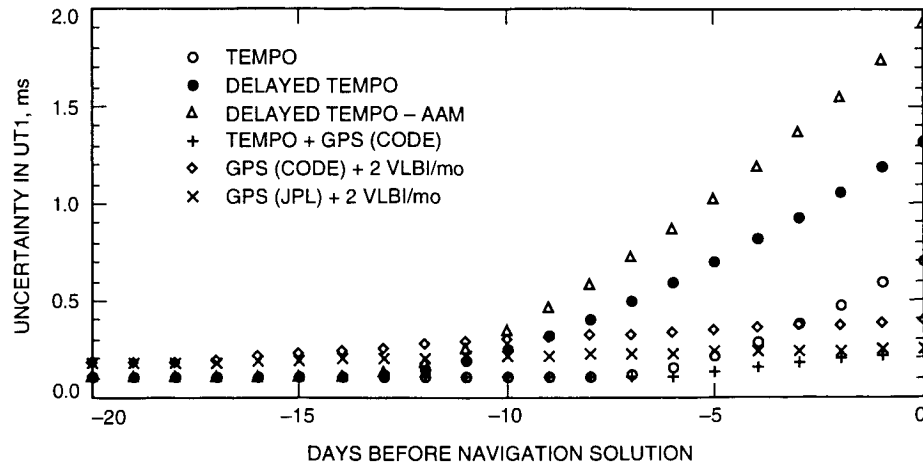


Fig. 2. Modeled UT1 errors versus time for six different calibration strategies.

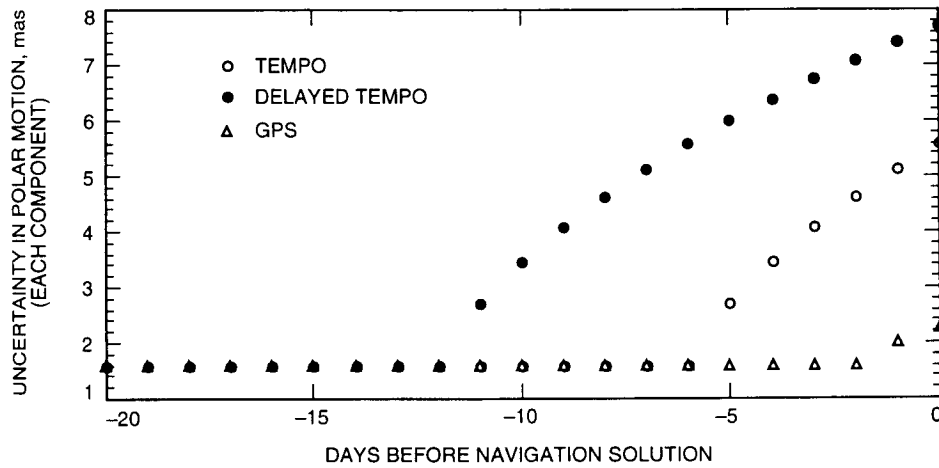


Fig. 3. Modeled polar motion errors versus time for three different calibration strategies.

Table 1. Earth orientation calibration accuracies for various strategies.

Calibration strategy	TAI - UT1 1-sigma, ms		Polar motion 1-sigma, mas	
	-21 days	0 days	-21 days	0 days
	TEMPO (current)	0.11	0.71	1.6
Delayed TEMPO	0.11	1.32	1.6	7.7
Delayed TEMPO - AAM	0.11	1.93	1.6	7.7
TEMPO + GPS (CODE)	0.11	0.23	1.6	2.3
GPS (CODE) + 2 VLBI/mo	0.18	0.39	1.6	2.3
GPS (JPL) + 2 VLBI/mo	0.18	0.25	1.6	2.3

quoted measurement uncertainties in order to accommodate possible offsets and drifts between various Earth orientation services.) In addition, the KEOF includes polar motion determinations from SLR measurements of Earth-orbiting satellites, which are available up to 5 days before the filter run (6 days before the navigation solution). The uncertainty in each component of polar motion was modeled as first-order Markov with a 5-day correlation time and a 1-sigma steady-state uncertainty of 1.6 mas, up to 6 days before the navigation solution, at which time the uncertainty was modeled as a random walk increasing to the final time. For times later than 6 days before the navigation solution, polar motion was modeled as a random walk that approximated the observed polar motion statistics [12]. (An integrated Gauss–Markov process was not used due to the difficulty in implementing it in the covariance analysis software.)

To investigate the importance of timely Earth orientation calibration delivery, two cases were included with a 6-day delay between the KEOF filter run and the navigation solution. The case labeled “delayed TEMPO” in Figs. 2 and 3 and in Table 1 is identical to the baseline case except for an additional 6-day delay. For the delayed TEMPO case, UT1 uncertainty is assumed to grow as an integrated random walk 13 days before the navigation solution, and polar motion begins to grow as a random walk 11 days before the navigation solution. A third case, labeled “delayed TEMPO – AAM,” is identical to the delayed TEMPO case except that AAM data in the KEOF solution are not included. Without the AAM data, the UT1 uncertainty begins growing as an integrated random walk 13 days prior to the navigation solution, but at a faster rate. The polar motion uncertainty is identical for those two cases, i.e., delayed TEMPO and delayed TEMPO – AAM.

Measurements of GPS satellites have been used extensively for geodetic purposes, and GPS data have a demonstrated capability to measure polar motion and LOD. (Recall LOD is directly related to UT1 rate.) For the past 2 years, the Center for Orbit Determination, Europe (CODE) has been producing daily measurements of polar motion and LOD with a week or more delay between data acquisition and Earth orientation delivery. There are plans for the DSN to begin rapid processing of GPS data to supplement and partially replace TEMPO VLBI measurements in an effort to reduce loading on the DSN’s 70-m subnetwork. If the measurements of LOD are uncorrelated (i.e., “white”), then including LOD measurements implies a random walk noise on UT1. Three cases of VLBI and GPS data combinations are included here assuming that the GPS LOD measurements are uncorrelated. The actual noise characteristics are under investigation. If the LOD measurements turn out to be correlated,¹¹ then the effect of GPS Earth orientation calibrations on navigation error may be different than the results presented in this article.

The fourth Earth orientation case, labeled “TEMPO + GPS(CODE),” assumes the current level of external VLBI measurements, the current two TEMPO VLBI passes each week, plus GPS polar motion and LOD measurements with a 1-day processing time. For this case, UT1 was assumed to behave as a Gauss–Markov process with a 5-day correlation time and a 1-sigma steady-state uncertainty of 0.11 ms until 7 days before the navigation solution, at which time the UT1 uncertainty was assumed to grow as a random walk at a level characteristic of the CODE GPS LOD deliveries. Each component of polar motion is described by a Gauss–Markov process with a 5-day correlation time and a 1.6-mas steady-state uncertainty (1-sigma) until 2 days before the navigation solution, at which time the polar motion uncertainty increases as a random walk. (This polar motion uncertainty model is assumed for all three cases that include GPS data.)

Because the current DSN plan is to utilize GPS LOD measurements so as to acquire fewer VLBI measurements, and because the number of external VLBI services has been steadily declining, the fifth Earth orientation case assumes that only two VLBI measurements are acquired per month and combined

¹¹ Preliminary studies of JPL GPS-derived LOD measurements exhibit “nonwhite” behavior on time scales longer than 3–5 days, A. P. Freedman, personal communication, Tracking Systems and Applications Section, Jet Propulsion Laboratory, Pasadena, California, August 18, 1995.

with GPS measurements. The case, labeled "GPS(CODE) + 2VLBI/mo" in the figures and in Table 1 assumes a 10-day delay in processing the VLBI measurements. This delay may occur as a result of reducing the load on the 70-m subnetwork, whereby VLBI measurements are acquired using the 34-m subnetwork. This strategy would require tapes to be used to record the VLBI data and shipped back to JPL for processing. With a 10-day delay between VLBI data acquisition and final processing, the latest VLBI measurement the KEOF could possibly include would be 11 days before the navigation solution with a worst-case delivery of 25 days before the navigation solution. For this case, it was assumed that the UT1 uncertainty behaved as a Gauss-Markov process with a 5-day correlation time and a 1-sigma steady-state uncertainty of 0.18 ms until 18 days prior to the navigation solution. This higher steady-state uncertainty is due to the lack of daily VLBI measurements from external services and reflects the uncertainty from using daily GPS LOD measurements to interpolate between VLBI UT1 measurements. At 18 days before the navigation solution, the UT1 uncertainty is assumed to grow as a random walk at a level characteristic of the CODE LOD measurements.

The current DSN plan is to have in place a JPL rapid GPS processing system for Earth orientation. The 3-year implementation cycle will begin in fiscal year 1996 with provisional operations beginning as early as fiscal year 1998. This will give way to a fully operational system by fiscal year 1999.¹² The processing implementation plan is under development but, as a test, there have been daily GPS solutions for LOD performed since late 1994. These solutions do not span a long enough time period to provide a good statistical measure of performance, but preliminary results indicate the JPL LOD measurements may be twice as accurate as the CODE deliveries. The sixth Earth orientation case, labeled "GPS(JPL) + 2VLBI/mo," is identical to the previous test case, GPS(CODE) + 2VLBI/mo, except that at 18 days before the navigation solution, the uncertainty in UT1 is assumed to begin a random walk behavior with a slower growth rate.

B. Mars Pathfinder Tracking and Error Modeling Assumptions

The Mars Pathfinder spacecraft will directly enter the Martian atmosphere from Earth transfer orbit for landing on the Martian surface. Other missions (e.g., Cassini, MGS) will either fly by the target planet or enter orbit through a series of orbital correction maneuvers. The primary atmospheric entry constraint for Mars Pathfinder is the flight path angle, the angle between the incoming velocity vector of the spacecraft and the vector normal to the Martian atmosphere. If this angle is too large (shallow), the spacecraft may overheat before parachute deployment, and if the angle is too small (steep), excess pressure may develop that could potentially damage the spacecraft's aeroshell from ablation. This entry angle constraint is expected to place the most stringent requirements on calibration of Earth orientation. A secondary requirement is to target the spacecraft to land within a predetermined landing footprint on the Martian surface. The size of the landing footprint is 100 km × 300 km.

The Mars Pathfinder spacecraft will be spin stabilized throughout its interplanetary cruise to Mars and will communicate through its high-gain antenna. The onboard telecommunications system has an X-band (7.2-GHz) uplink/X-band (8.4-GHz) downlink radio system, which will be used to acquire Doppler and ranging measurements and to transmit science and engineering telemetry data. The nominal launch window is a 30-day launch period beginning on December 5, 1996.¹³ Arrival at Mars is scheduled to occur on July 4, 1997. The launch vehicle will be targeted so that it will not impact the Martian surface. In the first 60 days after launch, two trajectory correction maneuvers (TCMs) will be performed to remove the effects of launch vehicle injection errors and to remove the targeting bias. A third TCM (TCM-3) is scheduled to be executed 60 days prior to Mars atmospheric entry. The critical navigation event time is just before the final maneuver (TCM-4). Five days prior to TCM-4, a navigation solution will be generated to design the final maneuver. The maneuver design command parameters will

¹²S. M. Lichten, personal communication, Tracking Systems and Applications Section, Jet Propulsion Laboratory, Pasadena, California, January 1995.

¹³At the time this article went to print, the actual launch window was not yet fixed since the mission profile and spacecraft launch mass were still being refined.

be uplinked to the spacecraft for execution from 10 to 15 days before atmospheric entry. Expected trajectory uncertainties for this critical navigation delivery have been carefully studied by Thurman and Kallemeyn^{14,15,16} via linear covariance analysis and Monte Carlo simulation. The covariance analysis assumptions adopted herein to assess the sensitivity of the critical Mars Pathfinder navigation solution to various Earth orientation calibration strategies were derived in large part from these earlier navigation performance assessments.

The nominal Mars Pathfinder trajectory is a so-called "Type I" trajectory, where the heliocentric longitude of the spacecraft changes by less than 180 deg between launch and arrival. An alternative "Type II" trajectory, where the heliocentric longitude of the spacecraft changes by more than 180 deg and less than 360 deg between launch and arrival, was originally considered for Mars Pathfinder. Analysts who first studied the Type II trajectory option suggest that the principal reasons the Type I trajectory option was preferred were (1) to attempt to minimize 70-m antenna conflicts between Mars Pathfinder at arrival and the Galileo mission at Jupiter, (2) to shorten the cruise time from ~11 months to ~7 months, which would yield less consumables in terms of propellant, and (3) to attain a more favorable geometry for the spacecraft to remain at Earth-point during cruise while maximizing the Sun's exposure to the solar arrays.¹⁷ (The Sun-probe-Earth angle is small for this mission.) A navigation error analysis for the Type II option was included in this assessment because some future missions to Mars (including MGS) will utilize Type II trajectories.

Table 2. Assumed data arc lengths for Mars Pathfinder navigation analysis.

Trajectory	Launch/arrival date	Data arc specification		
		Begin, days ^a	End, days ^b	Length, days
Type I	January 3, 1997/ July 4, 1997 (fixed)	$L + 60$	$M - 15$	107
Type II	December 2, 1996/ November 10, 1997 (fixed)	$L + 236$	$M - 15$	107

^a L = launch.
^b M = Mars arrival.

The tracking data arcs assumed for the covariance analysis are shown in Table 2 for both the Type I and Type II trajectories. X-band two-way coherent Doppler and ranging data were simulated over these intervals. DSN coverage varied according to the nominal DSN data acquisition schedule specified in the Mars Pathfinder *Navigation Plan*.¹⁸ For the Type I transfer phase ($L + 60$ days to $M - 45$ days), the DSN coverage was taken to be one 4-h pass/week per complex; during the Mars approach phase ($M - 45$ days to Mars arrival), continuous coverage was assumed; and for the TCM-3 phase, one 8-h pass/day (continuous for 12 h before and after TCM-3) was assumed over the interval $TCM \pm 3$ days. The same data arc

¹⁴ S. W. Thurman, "Orbit Determination Filter and Modeling Assumptions for MESUR Pathfinder Guidance and Navigation Analysis," JPL Interoffice Memorandum 314.3-1075 (internal document), Jet Propulsion Laboratory, Pasadena, California, October 15, 1993.

¹⁵ *Navigation Plan: Preliminary Version*, Pathfinder Flight Project, JPL D-11349 (internal document), Jet Propulsion Laboratory, Pasadena, California, December 1993.

¹⁶ *Navigation Plan: Critical Design Review Version*, Mars Pathfinder Project, JPL D-11349 (internal document), Jet Propulsion Laboratory, Pasadena, California, July 1994.

¹⁷ V. M. Pollmeier, personal communication, Navigation and Flight Mechanics Section, Jet Propulsion Laboratory, Pasadena, California, March 1995.

¹⁸ *Navigation Plan: Critical Design Review Version*, op. cit.

length was used for the Type II trajectory; thus, simulated data points began at $L + 236$ days. In an effort to minimize the effects of potential station or complex outages while maximizing the angle-finding capability of the ranging data, tracking passes were scheduled to alternate between DSN complexes.

The Doppler and ranging data were assumed to have measurement uncertainties of 0.09 mm/s (60 s average) and 2 m, respectively (1-sigma). Although recent X-band Doppler data residuals are typically smaller than 0.09 mm/s, a higher Doppler uncertainty was assumed in order to reflect the low-frequency power of the solar plasma noise spectrum that is not properly characterized by the root-mean-square of the residuals.¹⁹ A 20-min integration time was assumed for each data point (for both data types).

The Mars Pathfinder trajectories were integrated from initial position and velocity conditions (epoch state) using models for the dynamic forces on the spacecraft. The modeled gravitational forces were due to the masses of the Sun and the planets; relative locations of these bodies were based on the JPL DE200 ephemeris. Other forces modeled were nongravitational accelerations due to solar radiation pressure (SRP), gas leaks from valves and pressurized tanks, and attitude maintenance activity. In addition, TCM-3 maneuver execution errors were modeled.

Parameters estimated by the data reduction algorithm (a variant of the sequential Kalman filter [18]) included a wide array of dynamic and observational error sources categorized as (1) spacecraft epoch state, (2) spacecraft nongravitational force modeling errors, (3) maneuver execution errors, (4) errors in the orbital elements of the Earth and Mars, (5) systematic Doppler and ranging error biases, (6) transmission-media zenith delay calibration errors for the ionosphere and troposphere, (7) crust-fixed station location errors, and (8) Earth orientation calibration errors for UTPM. All of these error sources and their assumed a priori and steady-state values are summarized in Table 3. A priori uncertainties for the spacecraft initial state were large enough to leave it essentially unconstrained, while nongravitational forces were modeled as first-order Gauss-Markov random processes. (Note that all nongravitational forces except the slowly varying SRP accelerations were modeled using a stochastic gas leak model and are lumped under the category "NGA" in the table, where NGA denotes nongravitational accelerations.) TCM-3 execution errors (for the TCM-4 delivery) were modeled as random biases in all three body-fixed components. The uncertainty in the Earth-Mars ephemeris was taken from the JPL DE234 ephemeris error covariance by Standish,²⁰ but constrained with the knowledge that the orientation of the Earth's orbit is now known to 15 nrad [19]. For processing the two-way ranging data, the filter model included a bias parameter associated with each ranging pass from each station in order to approximate the slowly varying nongeometric delays in the ranging measurements that are caused principally by station delay calibration errors and uncalibrated solar plasma effects. The spacecraft spin rate, detectable in the Doppler signature, was estimated as a Gauss-Markov process with a 5-day correlation time. Uncertainty in knowledge of the station locations was assumed to be 10 cm for each component. This station location uncertainty is expected to be characteristic of the new DSN beam-waveguide (BWG) antennas once surveys are complete. More accurate station locations exist for antennas for which VLBI data are available, including the 70-m antennas and the 34-m high-efficiency (HEF) antennas.²¹

Although this study is restricted to the orbit determination problem and does not address the influence of guidance errors on navigational accuracy, it is important to note that, upon completion of TCM-4, the contribution of maneuver execution errors to the overall guidance dispersions are expected to be negligible. This was demonstrated in preflight error analyses and is discussed in greater detail in the Mars Pathfinder *Navigation Plan*.²²

¹⁹ W. M. Folkner, "Effect of Uncalibrated Charged Particles on Doppler Tracking," JPL Interoffice Memorandum 335.1-94-005 (internal document), Jet Propulsion Laboratory, Pasadena, California, March 1, 1994.

²⁰ E. M. Standish, "The JPL Planetary Ephemerides, DE234/LE234," JPL Interoffice Memorandum 314.6-1348 (internal document), Jet Propulsion Laboratory, Pasadena, California, October 8, 1991.

²¹ In actuality, the Mars Pathfinder spacecraft will be "uplink-limited" and will, therefore, require use of the 34-m HEF antennas for telecommunication. A more conservative assessment is made herein by assuming the 34-m BWG antennas.

²² *Navigation Plan: Critical Design Review Version*, op. cit.

Table 3. A priori and steady-state uncertainties for orbit determination error model parameters.

Estimated parameter set	Uncertainty, 1σ	Remarks
Spacecraft epoch state	A priori	Constant parameters
Position components	100 km	
Velocity components	1 m/s	
Nongravitational force model		
Solar radiation pressure (SRP)	Steady-state	First-order Markov
Radial (G_r)	5% of nominal	60-day correlation time
Transverse (G_x/G_y)	5% of nominal	
Gas leaks (NGA)	Steady-state	First-order Markov
Radial (a_r)	2×10^{-12} km/s ²	5-day correlation time
Transverse (a_x/a_y)	2×10^{-12} km/s ²	5-day correlation time
Maneuver execution error model		
TCM-3 ($\Delta V_x, \Delta V_y, \Delta V_z$) (for TCM-4 delivery)	A priori 10^{-2} m/s	Constant parameters
Planetary ephemerides error model		
Earth-Mars ephemeris	A priori	Constant parameters
Orbit orientation (3 Euler angles)	15 nrad	
Longitude with respect to periapsis	10 nrad	
Semimajor axis ($\Delta a/a$)	5 parts in 10^{11}	
Eccentricity (Δe)	3 parts in 10^{10}	
Ground system error model		
Range biases (one per station per pass)	A priori 1 m	Constant parameters
Transponder bias (ranging data only)	Steady-state 1 m	First-order Markov 0.5-day correlation time
Doppler spin bias (Doppler data only)	Steady-state 10^{-2} mm/s	First-order Markov 5-day correlation time
Transmission media	Steady-state	First-order Markov
Zenith troposphere	5 cm	0.1-day correlation time
Zenith ionosphere	5×10^{16} e/m ²	0.2-day correlation time
DSN station coordinates (crust-fixed r_s, z_h, λ)	A priori 10 cm	Constant parameters (uncorrelated)
Earth orientation	(cf., Section VI.A)	(cf., Section VI.A)
Timing (UT1)		
Polar motion (X,Y)		

C. Encounter Geometry

Because much of the strength of the Doppler and ranging data comes from the signature imposed by the rotation of the Earth, interpretation of the covariance analysis results is aided by understanding the encounter geometry.

The spacecraft position in the Earth–spacecraft direction is directly measured by ranging data. Doppler data help determine the other two components of the spacecraft position, which lie in the plane of the sky. There is a well-known weakness in determining spacecraft declination from Doppler data for spacecraft

near zero declination [1-3]. Spacecraft declination can be inferred from ranging data using tracking stations located in both northern and southern latitudes [20]. Figure 4 shows the Pathfinder Type I trajectory on the plane of the sky as viewed from Earth. As seen in the figure, encounter occurs near zero declination. Because of this encounter geometry, the spacecraft declination will probably depend upon ranging data, and the declination uncertainty should exhibit sensitivity to station delay calibration errors. In contrast, the Type II trajectory has a relatively large, negative encounter declination, as shown in Fig. 5. For the Type II encounter, the Doppler data will have a larger role in determining spacecraft declination, which should thus be less sensitive to station delay calibration errors.

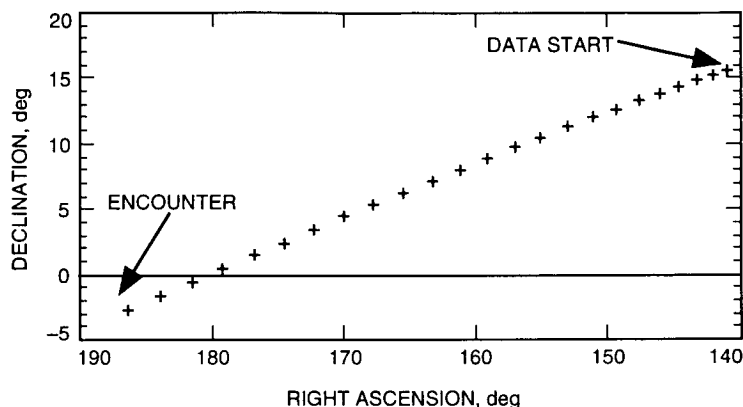


Fig. 4. Mars Pathfinder Type I trajectory as viewed from Earth; shown at 5-day intervals from the beginning of the data arc to encounter.

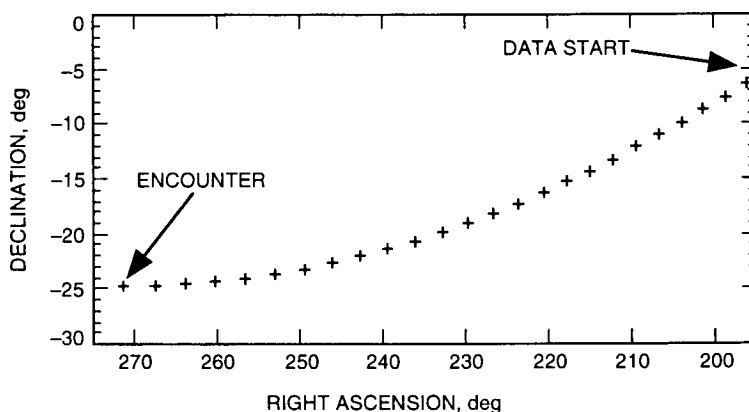


Fig. 5. Mars Pathfinder Type II trajectory as viewed from Earth; shown at 5-day intervals from the beginning of the data arc to encounter.

A typical uncertainty ellipsoid for the spacecraft position on approach would have principal axes approximately aligned with the plane-of-sky axes, with a much smaller uncertainty in the Earth-Mars direction than in the other two components (assuming ranging data are included). Planetary approach trajectories are typically described in aiming plane (B -plane) coordinates.²³ Figure 6(a) shows the relationship of the B -plane components to the plane-of-sky components for the Pathfinder Type I encounter. The approach direction, \hat{S} , is nearly parallel to the radial (Earth-Mars) direction, \hat{r} . The $-\hat{R}$ direction is in the plane normal to the approach direction, \hat{S} , and approximately parallel to the direction of increasing declination, $\hat{\delta}$, while the $-\hat{T}$ direction is in the plane normal to the approach direction and approximately

²³ For a complete description of the B -plane coordinate system, please refer to Appendix B.

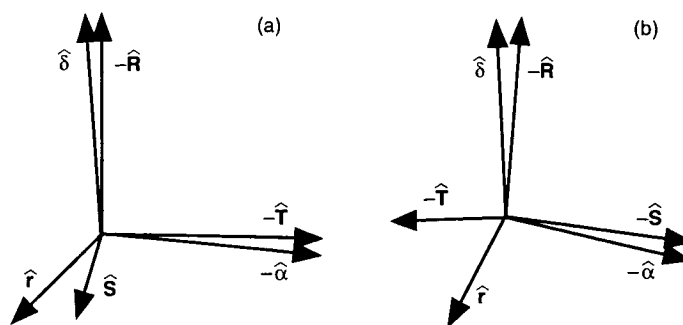


Fig. 6. The B -plane components for Mars Pathfinder approach trajectories with respect to plane-of-sky coordinates: (a) Type I and (b) Type II.

parallel to the direction of decreasing right ascension, $-\hat{\alpha}$. For the Type I trajectory, the well-determined component is approximately in the direction of approach. A small position uncertainty in this direction is expressed in the B -plane system as a small uncertainty in the time from encounter, i.e., linearized time of flight (LTOF). The position uncertainty is approximately related to the LTOF uncertainty by the approach velocity. For the Type I trajectory, the approach velocity is about 5.5 km/s (a 1-s uncertainty in LTOF corresponds to a position error of about 5.5 km). An error in right ascension, such as might be caused by a UT1 calibration error, will appear in the $B \cdot \hat{T}$ component.

Figure 6(b) shows the relationship of the B -plane components to the plane-of-sky components for the Type II trajectory. The direction of the spacecraft approach to Mars, $-\hat{S}$, is about 11 deg from the direction of decreasing right ascension, $-\hat{\alpha}$. The $-\hat{R}$ direction is about 23 deg from the declination axis, $\hat{\delta}$. The $-\hat{T}$ direction is about 23 deg from the Earth-Mars direction, \hat{r} . For this trajectory, an error in right ascension will be reflected mainly in LTOF. For the Type II trajectory, the approach velocity is approximately 3.9 km/s.

Mars Pathfinder navigation is required to deliver, prior to the final maneuver (TCM-4), a trajectory estimate with less than a 1-percent probability of exceeding the entry angle requirement. The latest assessment of the Type I flight path entry angle requirement is ± 1 deg (99 percent), which implies a requirement on the navigation delivery corresponding to a 3-sigma uncertainty of 21 km in the magnitude of the impact parameter.²⁴ Stated another way, the entry corridor is 42-km wide, as depicted in Fig. 7.

D. Results

In the covariance studies performed, a careful model was constructed for the time-dependent Earth orientation errors shown in Figs. 2 and 3. This model would be somewhat difficult to implement into the operational Orbit Determination Program (ODP),²⁵ which currently does not have a statistical reset capability or an integrated random walk model such as the one used in this analysis. Because of this limitation, the effect of each Earth orientation calibration strategy on the total orbit determination error was calculated in two ways. For the first estimation method, the contribution to orbit determination error from Earth orientation was determined with UT1 and polar motion included (i.e., estimated) in the navigation solution, with correctly modeled time-dependent a priori uncertainties. In the second estimation method, the contribution to orbit determination error was assessed under the assumption that the Earth orientation calibration errors were ignored (i.e., not estimated) in the navigation solution.

²⁴ P. K. Kallemeyn, personal communication, Navigation and Flight Mechanics Section, Jet Propulsion Laboratory, Pasadena, California, March 1995.

²⁵ The ODP is a large institutional software system used for research and navigation support of flight operations, N. D. Panagiotopoulos, J. W. Zielenbach, and R. W. Duesing, *An Introduction to JPLs Orbit Determination Program*, JPL 1846-37 (internal document), Jet Propulsion Laboratory, Pasadena, California, May 21, 1974.

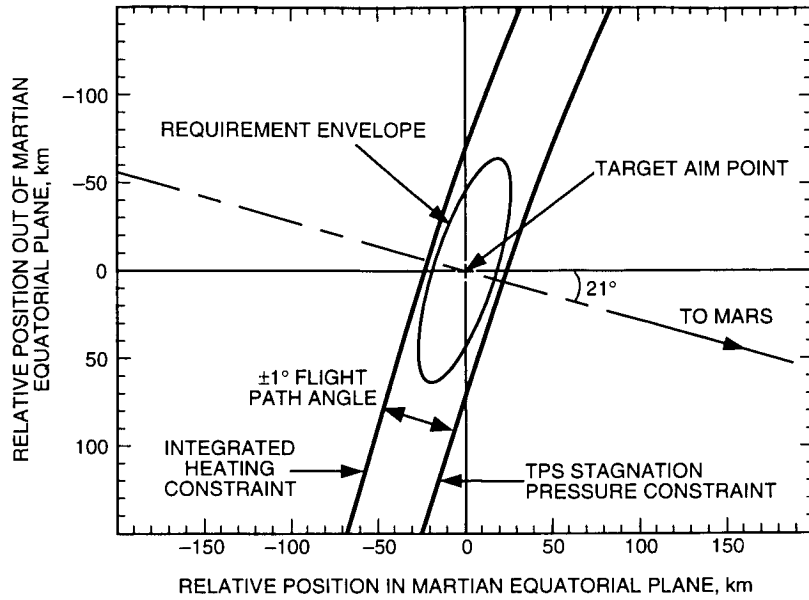


Fig. 7. Mars Pathfinder entry corridor and landing accuracy requirements (99 percent). (Note: the Earth equatorial plane is nearly parallel to the direction to Mars.)

Figure 8 shows the contribution to the total navigational uncertainty for the nominal (Type I) Mars Pathfinder trajectory from all error sources described in Section VI.B except Earth orientation. The covariance analysis results given below are expressed in B -plane components referred to the Earth mean equator of J2000 (EME2000), as described in Appendix B. Contributions were computed in a manner such that the sum of each error source, when added in quadrature, gives the total navigation uncertainty in a root-sum-square sense [21]. The critical navigation parameter for Pathfinder approach is the magnitude of the impact parameter, denoted $|\mathbf{B}|$. Recall from the previous discussion that $|\mathbf{B}|$ is related to the flight path entry angle. For the nominal Pathfinder Type I approach trajectory, the $\mathbf{B} \cdot \hat{\mathbf{T}}$ uncertainty, denoted $\sigma_{\mathbf{B} \cdot \hat{\mathbf{T}}}$, is nearly the same as the uncertainty in $|\mathbf{B}|$. In general, the relationship of the component uncertainties $\sigma_{\mathbf{B} \cdot \hat{\mathbf{R}}}$, $\sigma_{\mathbf{B} \cdot \hat{\mathbf{T}}}$, and $\sigma_{|\mathbf{B}|}$ depends upon the choice of the targeted entry point.

The uncertainties in arrival time (LTOF) are very small because of the approach direction nearly coinciding with the Earth–Mars direction, which is well determined by ranging data. The scale for LTOF in Fig. 8(c) is 3 s and corresponds to a position uncertainty of about 15 km. The major error source (other than Earth orientation) for $\mathbf{B} \cdot \hat{\mathbf{T}}$ (\sim right ascension) is the anomalous nongravitational accelerations (NGAs). The $\mathbf{B} \cdot \hat{\mathbf{R}}$ (\sim declination) uncertainty has roughly equal contributions from data noise, nongravitational forces, and station delay calibrations for ranging data. The 1-m accuracy of the range bias calibrations assumed for the covariance analysis has been inferred from observations of the day-to-day consistency of Mars Observer ranging data residuals [22]. This assumption should be interpreted cautiously since the systematic effects in the Mars Observer range biases could have been absorbed by other spacecraft trajectory parameters, such as nongravitational accelerations. Fortunately, this is not an issue for Mars Pathfinder since the critical navigation component, $|\mathbf{B}|$, is almost entirely in the right ascension direction. Further, this navigation error analysis was not intended to be the “official” Mars Pathfinder analysis. The principal purpose here was to provide a quantitative measure of the relative importance of potential error sources, specifically, Earth orientation calibration errors.

Figure 9 illustrates the contribution to the total orbit determination uncertainty from each case of Earth orientation calibration error described in Section VI.A. Here, it is seen that Earth orientation calibration errors are a significant source of error for Mars Pathfinder in the critical $\mathbf{B} \cdot \hat{\mathbf{T}}$ and $|\mathbf{B}|$

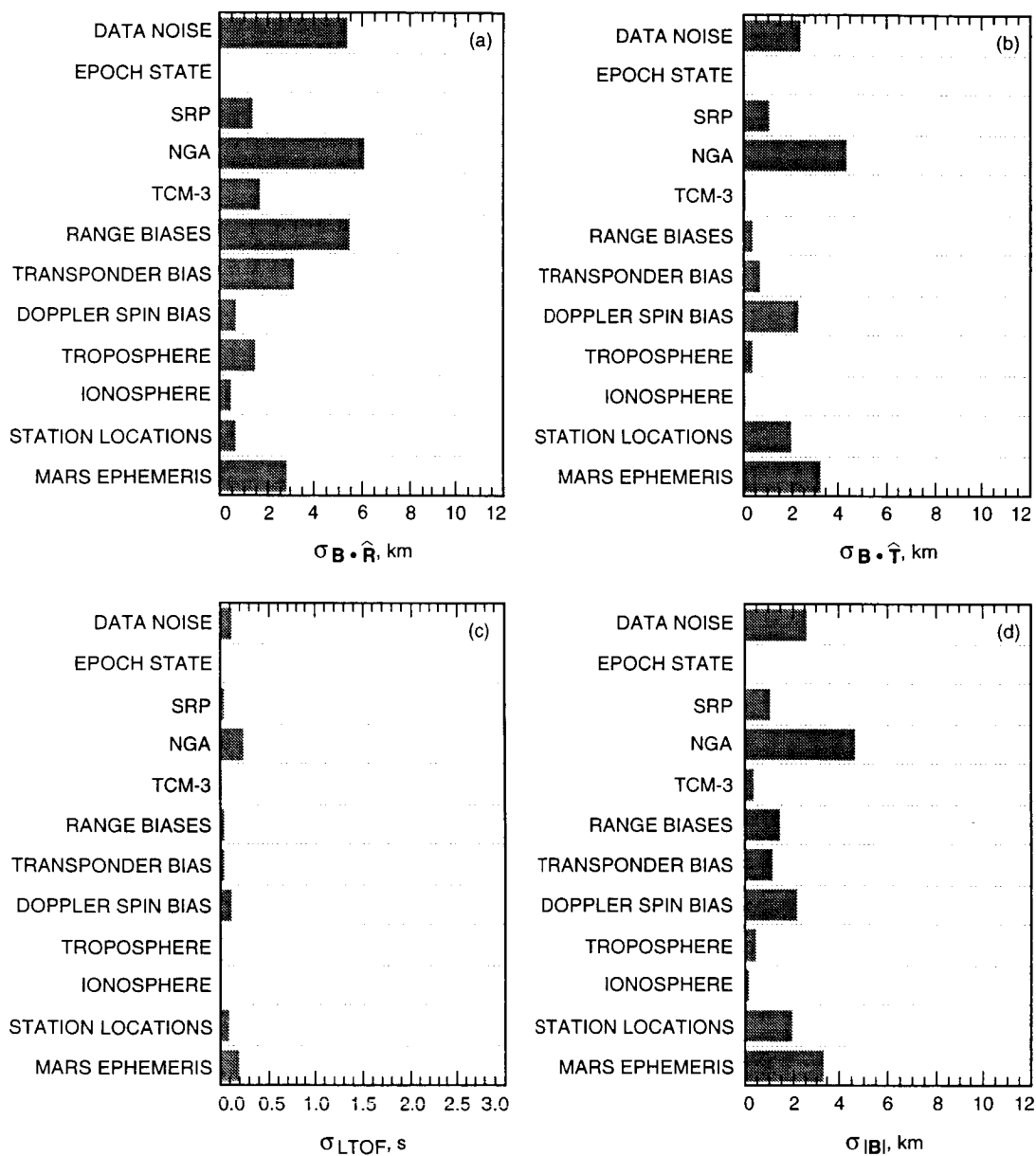


Fig. 8. Relative contributions of the principal error sources (other than Earth orientation) to the total Mars Pathfinder orbit determination uncertainty. Uncertainties are shown in B -plane coordinates with respect to the mean Earth equator of 2000: (a) $\mathbf{B} \cdot \hat{\mathbf{R}}$ (\sim declination) uncertainty, (b) $\mathbf{B} \cdot \hat{\mathbf{T}}$ (\sim right ascension) uncertainty, (c) LTOF (time of encounter) uncertainty, and (d) uncertainty in the magnitude of the impact parameter, $|\mathbf{B}|$.

components.²⁶ Earth orientation calibration error is less significant in the $\mathbf{B} \cdot \hat{\mathbf{R}}$ and LTOF components. The lack of sensitivity to Earth orientation in the LTOF direction is due to the fact that the approach direction is nearly aligned with the Earth–Mars direction; therefore, LTOF is well determined by the ranging data. The spacecraft declination (nearly aligned with the $\mathbf{B} \cdot \hat{\mathbf{R}}$ direction) is determined largely by ranging data at northern and southern latitude stations since, at the low encounter declination, the Doppler data do not contribute much to the determination of declination. Because the declination is

²⁶ Recall that errors due to precession and nutation were neglected from this analysis; thus, the formal Earth orientation calibration errors are strictly due to UTPM calibration errors.

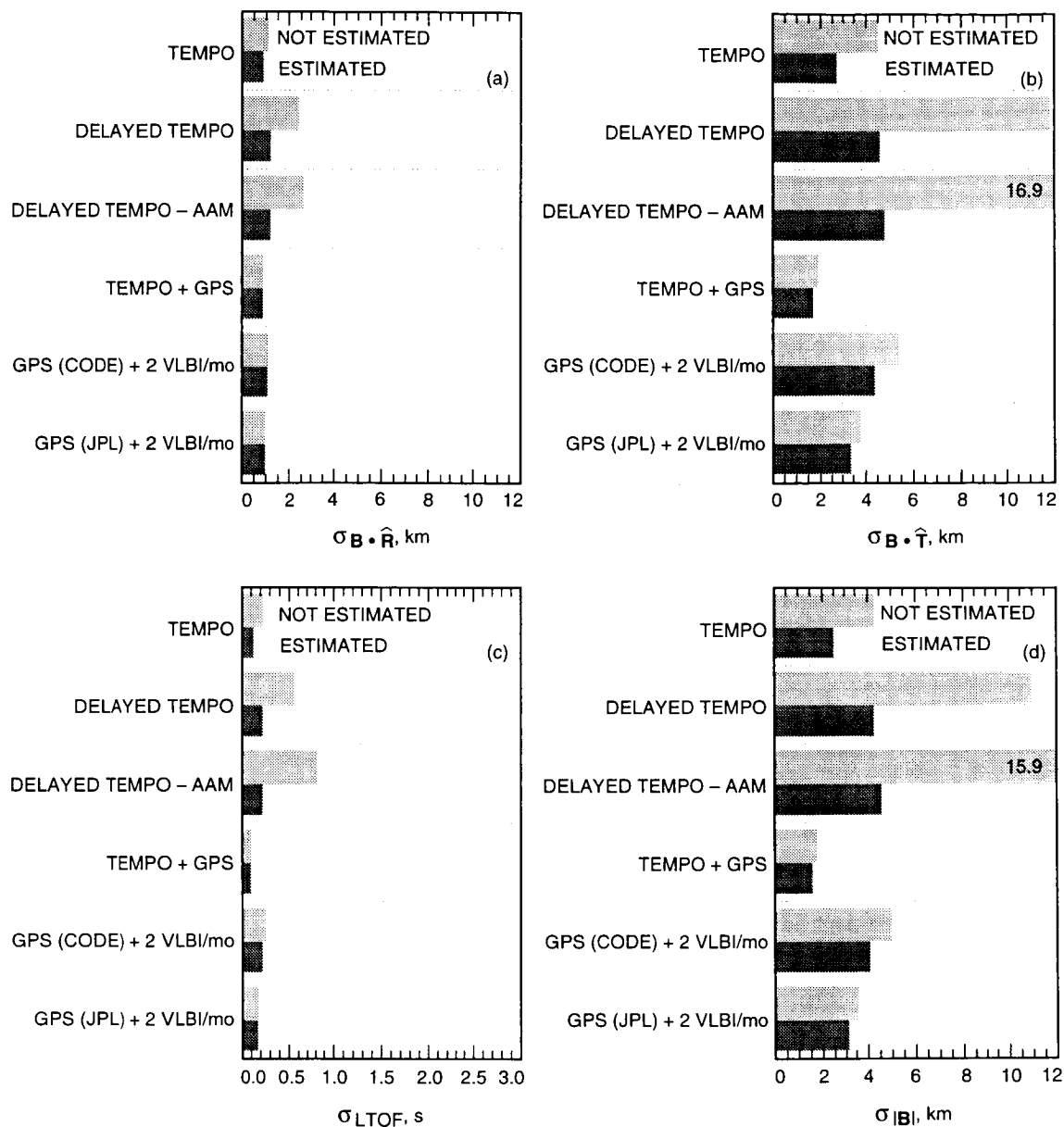


Fig. 9. Relative contributions of Earth orientation to the total Mars Pathfinder orbit determination uncertainty. Uncertainties are shown in B -plane coordinates with respect to the mean Earth equator of 2000: (a) $\mathbf{B} \cdot \hat{\mathbf{R}}$ (-declination) uncertainty, (b) $\mathbf{B} \cdot \hat{\mathbf{T}}$ (-right ascension) uncertainty, (c) LTOF (time of encounter) uncertainty, and (d) uncertainty in the magnitude of the impact parameter, $|\mathbf{B}|$. Uncertainties are given for both the case where Earth orientation parameters were estimated in the navigation solutions and for cases where Earth orientation was not adjusted in the navigation solution.

determined principally by ranging data with an assumed accuracy of 1 m, there is not much sensitivity to Earth orientation errors for the calibration strategies studied here, which all give Earth orientation errors smaller than 1 m at the Earth's surface.

In the case of current DSN Earth orientation calibration performance, assuming a delivery of the calibration files on the day of the critical navigation solution from TEMPO VLBI data, Fig. 9(d) shows that Earth orientation errors contribute approximately 39 percent of the 1-sigma $|\mathbf{B}|$ (flight path entry angle) requirement of 7 km for the case where UTPM parameters were included in the navigation solution,

and 64 percent of the allowable error if UTPM were ignored in the navigation solution. The two Earth orientation calibration cases with delayed delivery show contributions to navigation uncertainty that are significantly larger. The delayed calibration cases are most likely unacceptable for the Mars Pathfinder mission. The optimistic Earth orientation case, in which the current twice-weekly TEMPO VLBI measurements are augmented with daily GPS data, shows a much smaller contribution to the navigation uncertainty than the nominal TEMPO case. The two calibration strategies with daily GPS data combined with reduced VLBI observations (2 VLBI/month) are comparable to the nominal TEMPO case. In contrast to the nominal TEMPO case, the GPS-based calibrations exhibit smaller differences between the strategy of including UTPM parameters and statistics in the navigation solution and the strategy of ignoring the UTPM parameters in the navigation solution.

Figure 9 shows a reduced sensitivity to Earth orientation errors when the UTPM parameters are estimated, along with the trajectory parameters, in the navigation filter. This improvement is large for the cases with poorest UTPM accuracy. The improvement is coupled to the assumptions about the level of nongravitational forces affecting the spacecraft. If there were no nongravitational forces acting on the spacecraft, or if the nongravitational forces were perfectly known, then the spacecraft would provide a reference against which Earth orientation changes could be measured using Doppler data. If there were large nongravitational forces affecting the spacecraft that are not well known, then the spacecraft could not be used as a reference against which Earth orientation changes could be measured. Because the Pathfinder spacecraft will be a simple, spinning platform, the nongravitational forces affecting it are assumed here to be well modeled. Because of this assumption, when the Earth orientation uncertainties increase beyond a certain level, the navigation filter begins to rely on the assumed level of nongravitational force uncertainties and can improve upon the a priori knowledge assumed for Earth orientation parameters. This would not be true for a spacecraft with larger uncertainties in the nongravitational force model.

Because of the different encounter geometry, the covariance analysis results for the Type II trajectory are quite different from the Type I trajectory. No attempt was made to quantify the critical navigation component, $|\mathbf{B}|$, since the Type II trajectory will not be used for Mars Pathfinder and the choice of the targeted point for this study was arbitrary. The B -plane component uncertainties should be interpreted in such a manner that the critical component could be more like $\mathbf{B} \cdot \hat{\mathbf{R}}$ or $\mathbf{B} \cdot \hat{\mathbf{T}}$, depending on the choice of the targeted point.

Figure 10 shows the navigation uncertainty from all error sources for the Type II trajectory with the exception of Earth orientation calibration error. The LTOF uncertainty is about a factor of six larger for the Type II case than for the Type I case because the approach direction is not aligned with the Earth–Mars direction. The scale in Fig. 10(c), 3 s, corresponds to a position uncertainty of about 12 km due to the approach velocity of 3.9 km/s. Nongravitational forces, Mars ephemeris uncertainty, and data noise are seen to be the dominant sources of error (other than Earth orientation) for the other components. The $\mathbf{B} \cdot \hat{\mathbf{T}}$ component is most closely aligned with the Earth–Mars direction at encounter and, hence, is the best determined component. The uncertainty in $\mathbf{B} \cdot \hat{\mathbf{R}}$ (\sim declination) shown in Fig. 10(a) for the Type II trajectory is less sensitive to ranging calibration errors and more sensitive to station location errors than is the Type I case. This is a reflection of the large, negative encounter declination enabling Doppler data to influence the determination of declination.

Figure 11 shows the contribution of Earth orientation calibration errors to the orbit determination uncertainty for the Type II trajectory. The $\mathbf{B} \cdot \hat{\mathbf{R}}$ uncertainty is much more dependent on Earth orientation than is the Type I case. This sensitivity is related to the determination of declination by the Doppler data, which are sensitive to Earth platform errors. The sensitivity of declination to Earth orientation can be seen to be principally due to polar motion errors since cases with identical polar motion uncertainties, but different UT1 uncertainties, have the same effect on the $\mathbf{B} \cdot \hat{\mathbf{R}}$ uncertainty. The $\mathbf{B} \cdot \hat{\mathbf{T}}$ component shows some sensitivity to UT1 errors since the $\hat{\mathbf{T}}$ direction is mostly in the Earth–Mars direction but partly in the direction of increasing right ascension. UT1 errors have a larger effect on LTOF since the

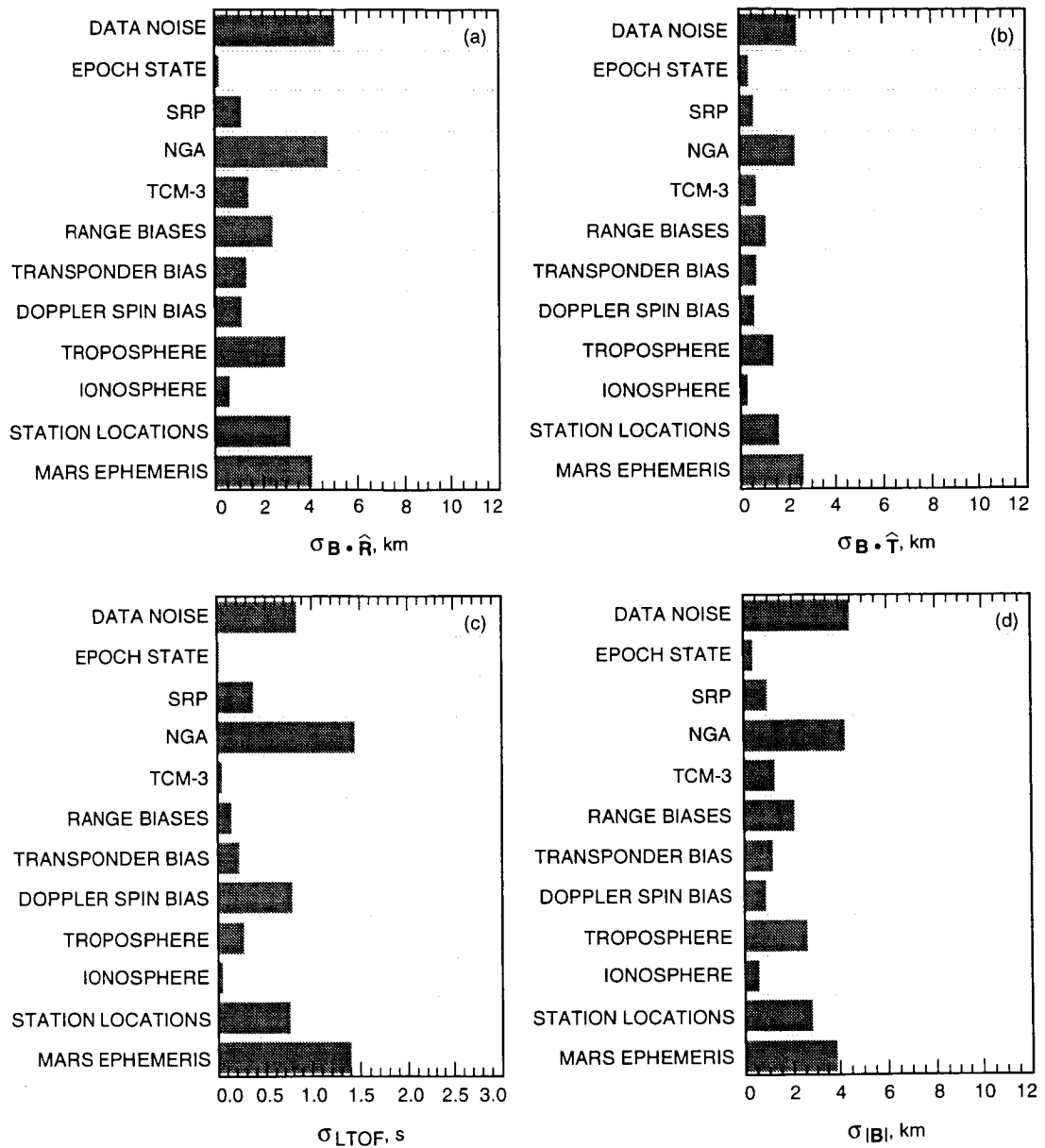


Fig. 10. Relative contributions of the principal error sources (other than Earth orientation) to the total orbit determination uncertainty for a Mars Pathfinder Type II approach scenario. Uncertainties are shown in B -plane coordinates with respect to the mean Earth equator of 2000: (a) $\mathbf{B} \cdot \hat{\mathbf{R}}$ (-declination) uncertainty, (b) $\mathbf{B} \cdot \hat{\mathbf{T}}$ (-right ascension) uncertainty, (c) LTOF (time of encounter) uncertainty, and (d) uncertainty in the magnitude of the impact parameter, $|\mathbf{B}|$.

approach direction is more closely aligned with the right ascension direction. The nominal TEMPO Earth orientation errors would be one of the larger sources for error in $\mathbf{B} \cdot \hat{\mathbf{T}}$ and a moderate source of error in $\mathbf{B} \cdot \hat{\mathbf{R}}$ for this trajectory. The GPS-based cases contribute less to the navigation uncertainty in $\mathbf{B} \cdot \hat{\mathbf{R}}$ and $\mathbf{B} \cdot \hat{\mathbf{T}}$ than the nominal TEMPO case, but result in large errors in LTOF.

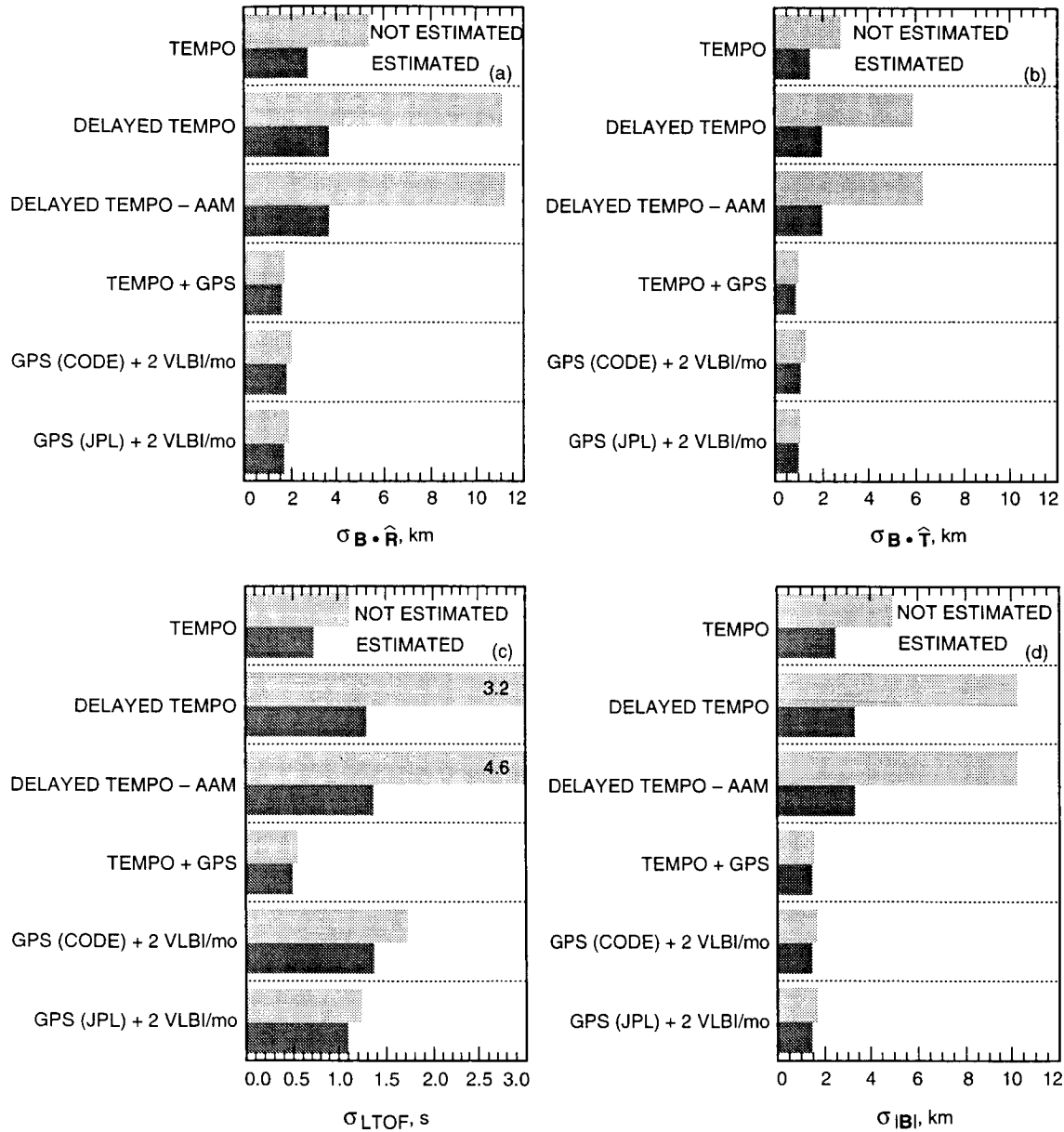


Fig. 11. Relative contributions of Earth orientation for a Mars Type II approach trajectory. Uncertainties are shown in B -plane coordinates with respect to the mean Earth equator of 2000: (a) $B \cdot \hat{R}$ (~declination) uncertainty, (b) $B \cdot \hat{T}$ (~right ascension) uncertainty, (c) LTOF (time of encounter) uncertainty, and (d) uncertainty in the magnitude of the impact parameter, $|B|$. Uncertainties are given for both the case where Earth orientation parameters were estimated in the navigation solutions and for cases where Earth orientation was not adjusted in the navigation solution.

VII. Summary and Conclusions

A numerical assessment measuring the sensitivity of spacecraft delivery errors to the accuracy and timeliness of Earth orientation calibrations was completed for two interplanetary cruise scenarios derived from the Mars Pathfinder mission set. This study was motivated by the fact that, to date, errors in Earth orientation (i.e., precession/nutation, polar motion, and variation in Earth rotation rate) are still capable

of contributing significantly to the composition of the noise signature on radio metric data acquired by the DSN. These errors can thus lead to degraded spacecraft navigational accuracies if not adequately calibrated.

Results from the navigation sensitivity analysis concurred with the expected outcome that not only is Earth orientation calibration performance important in determining spacecraft navigational accuracy, but so is the timeliness of the calibration file deliveries. Based on the analyses presented in this article, the current best DSN Earth orientation calibration performance provided by the TEMPO activity yielded a contribution of about 39 to 64 percent of the total navigation error budget for the critical component of the nominal Mars Pathfinder Type I trajectory, depending on the navigation filtering strategy being used. These results assumed line-of-sight data types (i.e., two-way Doppler and range) were used in the navigation process. Use of differential data types could reduce the sensitivity to Earth orientation calibration errors.

Variations on the current DSN calibration method representing delayed TEMPO deliveries of the calibration files as well as delayed deliveries without use of AAM data were also assessed. Results for these cases showed that Earth orientation calibration errors dominated the total navigation error budget, irrespective of the trajectory type. Furthermore, a very large penalty was paid when the Earth orientation parameters were not adjusted in the navigation solution.

With the advent of GPS-based ground observations as a viable Earth orientation calibration system and the ongoing effort to reduce the loading on the DSN 70-m subnetwork, new Earth orientation calibration techniques are being devised. Statistical models representing examples of these calibration strategies were constructed and their effect on the Mars Pathfinder navigation delivery error assessed. In the (optimistic) case where the current level of TEMPO calibrations (2 per week) was used in concert with daily GPS-based calibrations, the influence of UTPM calibration errors on overall navigation performance was, as expected, minimal. Under the current environment where there is continual pressure to reduce the number of DSN-based VLBI observations (again, addressing the 70-m antenna loading issue), this calibration strategy will probably not be attainable operationally.

A sensitivity analysis was also performed for an operationally more realistic Earth orientation calibration strategy in which GPS-based calibrations were used as the principal means of generating frequent (daily) Earth orientation calibration information, augmented with periodic VLBI-based measurements (~ 2 per month). (The GPS system alone cannot determine all components of Earth orientation and, thus, requires an external calibration source such as VLBI.) In this assessment, analysis results suggest that the contribution of UTPM errors to the total navigation error budget for the critical component of the nominal Mars Pathfinder trajectory lies somewhere between 43 and 55 percent, depending on the accuracy of the GPS deliveries. These results assumed that the UTPM parameters were adjusted in the navigation solution. The true level of accuracy will depend, of course, on the actual system implemented.

Since the GPS calibration system is in the early stages of development, the statistical characteristics of the calibrations are not yet well determined. With the noise levels assumed for this analysis, the GPS-based Earth orientation calibrations appear to offer an advantage over the current TEMPO-based calibrations in that they relax the need for the navigation process to properly model the time-varying behavior of UTPM calibration errors. In addition, the proposed system is designed to provide rapid processing and timely deliveries of the calibration files to the flight projects. The overall performance (accuracy) levels, as evidenced in this study, were at or near the same level as the current DSN capability, perhaps only slightly better in some cases.

Acknowledgments

The authors would like to thank the following individuals, who greatly assisted in preparation of this article: Alan Steppe, who graciously agreed to referee this article and assisted with several excellent technical discussions regarding correct statistical modeling of the Earth orientation calibration errors; Adam Freedman, who helped determine the level of uncertainty to assign to each Earth orientation calibration strategy; Carl Christensen, Jean Dickey, Tom Runge, Jim Border, and George Resch for providing a number of useful technical comments based on early drafts of this article; and Pieter Kallemeyn and Vince Pollmeier for the frequent tutorial sessions on the Mars Pathfinder mission. Without the help of all of these individuals, this research task could not have been accomplished.

It is hoped that this article will assist future mission study teams and end users in the understanding of errors associated with the DSN Earth orientation calibration process and the potential limiting effect these errors can have on spacecraft radio navigation performance.

References

- [1] J. O. Light, "An Investigation of the Orbit Redetermination Process Following the First Mid-Course Maneuver," *Supporting Research and Advanced Development, Space Programs Summary 37-33*, vol. IV, Jet Propulsion Laboratory, Pasadena, California, pp. 8-17, June 30, 1965.
- [2] T. W. Hamilton and W. G. Melbourne, "Information Content of a Single Pass of Doppler Data From a Distant Spacecraft," *The Deep Space Network, Space Programs Summary 37-39*, vol. III, Jet Propulsion Laboratory, Pasadena, California, pp. 18-23, May 31, 1966.
- [3] D. W. Curkendall and S. R. McReynolds, "A Simplified Approach for Determining the Information Content of Radio Tracking Data," *Journal of Spacecraft and Rockets*, vol. 6, no. 5, pp. 520-525, May 1969.
- [4] N. A. Renzetti, editor, *A History of the Deep Space Network: From Inception to January 1, 1969*, JPL Technical Report 32-1533, vol. I, Jet Propulsion Laboratory, Pasadena, California, September 1, 1971.
- [5] P. K. Seidelmann, "1980 IAU Theory of Nutation: The Final Report of the IAU Working Group on Nutation," *Celestial Mechanics*, vol. 27, pp. 19-106, 1982.
- [6] A. P. Freedman, J. A. Steppe, J. O. Dickey, T. M. Eubanks, and L.-Y. Sung, "The Short-Term Prediction of Universal Time and Length of Day Using Atmospheric Angular Momentum," *Journal of Geophysical Research*, vol. 99, no. B4, pp. 6981-6996, April 10, 1994.
- [7] T. A. Herring, B. A. Buffett, P. M. Mathews, and I. I. Shapiro, "Forced Nutations of the Earth: Influence of Inner Core Dynamics 3. Very Long Interferometry Data Analysis," *Journal of Geophysical Research*, vol. 96, pp. 8259-8273, 1991.
- [8] P. Charlot, O. J. Sovers, J. G. Williams, and X X Newhall, "Precession and Nutation From Joint Analysis of Radio Interferometric and Lunar Laser Ranging Observations," *Astronomical Journal*, vol. 109, pp. 418-427, 1995.

- [9] J. A. Steppe, S. H. Oliveau, and O. J. Sovers, "Earth Rotation Parameters From DSN VLBI: 1994," *IERS Technical Note 17*, Observatoire de Paris, Paris, France, pp. R19-R32, 1994.
- [10] J. H. Lieske, T. Lederle, W. Fricke, and B. Morando, "Expressions for the Precession Quantities Based Upon the IAU (1976) System of Astronomical Constants," *Astronomy and Astrophysics*, vol. 58, pp. 1-16, 1977.
- [11] J. H. Lieske, "Precession Matrix Based on IAU (1976) System of Astronomical Constants," *Astronomy and Astrophysics*, vol. 73, pp. 282-284, 1979.
- [12] D. D. Morabito, T. M. Eubanks, and J. A. Steppe, "Kalman Filtering of Earth Orientation Changes," *Earth's Rotation and Reference Frames for Geodesy and Geodynamics*, edited by A. K. Babcock and G. A. Wilkins, Dordrecht, Holland: D. Riedel, pp. 257-267, 1988.
- [13] N. A. Renzetti, J. F. Jordan, A. L. Berman, J. A. Wackley, and T. P. Yunck, *The Deep Space Network—An Instrument for Radio Navigation of Deep Space Probes*, JPL Publication 82-102, Jet Propulsion Laboratory, Pasadena, California, pp. 77-78 and 88-91, December 15, 1982.
- [14] H. F. Fliegel and R. N. Wimberly, "Time and Polar Motion," *Tracking System Analytic Calibration Activities for the Mariner Mars 1971 Mission*, JPL Technical Report 32-1587, Jet Propulsion Laboratory, Pasadena, California, pp. 77-81, March 1, 1974.
- [15] D. W. Trask and P. M. Muller, "Timing: DSIF Two-Way Doppler Inherent Accuracy Limitations," *The Deep Space Network, Space Programs Summary 37-39*, vol. III, Jet Propulsion Laboratory, Pasadena, California, pp. 7-16, May 31, 1966.
- [16] P. M. Muller and C. C. Chao, "Timing Errors and Polar Motion," *Tracking System Analytic Calibration Activities for the Mariner Mars 1969 Mission*, JPL Technical Report 32-1499, Jet Propulsion Laboratory, Pasadena, California, pp. 35-43, November 15, 1970.
- [17] J. F. Jordan, G. A. Madrid, and G. E. Pease, "Effects of Major Errors Sources on Planetary Spacecraft Navigation Accuracies," *Journal of Spacecraft and Rockets*, vol. 9, no. 3, pp. 196-204, March 1972.
- [18] G. J. Bierman, *Factorization Methods for Discrete Sequential Estimation*, San Diego, California: Academic Press, Inc., 1977.
- [19] W. M. Folkner, P. Charlot, M. H. Finger, J. G. Williams, O. J. Sovers, X X Newhall, and E. M. Standish, Jr., "Determination of the Extragalactic-Planetary Frame Tie From Joint Analysis of Radio Interferometric and Lunar Laser Ranging Measurements," *Astronomy and Astrophysics*, vol. 287, pp. 279-289, 1994.
- [20] S. W. Thurman, T. P. McElrath, and V. M. Pollmeier, "Short-Arc Orbit Determination Using Coherent X-Band Ranging Data," *Advances in the Astronautical Sciences*, vol. 79, part I, pp. 23-44, 1992.
- [21] J. A. Estefan and P. D. Burkhart, "Enhanced Orbit Determination Filter Sensitivity Analysis: Error Budget Development," *The Telecommunications and Data Acquisition Progress Report 42-116, October-December 1993*, Jet Propulsion Laboratory, Pasadena, California, pp. 24-36, February 15, 1994.
- [22] L. A. Cangahuala, E. J. Graat, D. C. Roth, S. W. Demcak, P. B. Esposito, and R. A. Mase, "Mars Observer Interplanetary Cruise Orbit Determination," *Advances in the Astronautical Sciences*, vol. 87, part II, pp. 1049-1068, 1994.

- [23] L. J. Wood, "Orbit Determination Singularities in the Doppler Tracking of a Planetary Orbiter," *Journal of Guidance, Control, and Dynamics*, vol. 9, no. 4, pp. 485-494, July-August 1986.
- [24] D. B. Engelhardt, J. B. McNamee, S. K. Wong, F. G. Bonneau, E. J. Graat, R. J. Haw, G. R. Kronschnabl, and M. S. Ryne, "Determination and Prediction of Magellan's Orbit," *Advances in the Astronautical Sciences*, vol. 75, part II, pp. 1143-1160, 1991.
- [25] S. W. Thurman, "Information Content of Interferometric Delay-Rate Measurements for Planetary Orbiter Navigation," paper AIAA-90-2909, AIAA/AAS Astroynamics Conference, Portland, Oregon, August 20-22, 1990.
- [26] J. D. Giorgini, E. J. Graat, T.-H. You, M. S. Ryne, S. K. Wong, and J. B. McNamee, "Magellan Navigation Using X-Band Differenced Doppler During Venus Mapping Phase," paper AIAA-92-4521, AIAA/AAS Astroynamics Conference, Hilton Head, South Carolina, August 10-12, 1992.
- [27] W. Kizner, *A Method of Describing Miss Distances for Lunar and Interplanetary Trajectories*, JPL Publication 674, Jet Propulsion Laboratory, Pasadena, California, August 1, 1959.

Appendix A

Sensitivity of Planetary Orbiter Navigation to Earth Orientation—A Case Study for Differential Data Types

For a spacecraft in orbit about another planet, Doppler data can be used to determine all components of its orbit except for a few particular geometries [23]. The accuracy with which the orbit is determined by means of Earth-based Doppler tracking depends upon several factors, including data accuracy and the accuracy of the spacecraft force models, particularly those due to the planet's gravitational field. Using the Magellan radar mapping mission of Venus as an example, the uncertainty of the gravity field was such that the expected orbit uncertainty during the prime mission (for daily orbit solutions) was about 15 km with two-way Doppler tracking alone [24]. Mars Global Surveyor (MGS) plans to achieve much better accuracy by solving for an improved gravity field based on an initial data set. The MGS strategy could not have been utilized for Magellan since the gravity field of Venus could not be sampled with a few weeks of radio metric data because of Venus' slow rotation rate.

The orbit determination accuracy achievable with Earth-based Doppler tracking in a two-way coherent mode is very insensitive to Earth orientation errors since the dominant signature in the Doppler data is due to the orbit of the spacecraft about the planet. This is in contrast to planetary approach navigation, where much of the information content in Doppler tracking data is influenced by the Earth's rotation. To first order, Doppler data are insensitive to a rotation about the line of sight from the Earth-based tracking station to the spacecraft. The rotation about the line of sight can be determined by changes in the geometry due to the relative orbits of the Earth and the target planet about which the spacecraft is orbiting. Rotation about the line of sight is measured by the node angle, Ω , with respect to the plane of the sky, which is defined in Fig. A-1 as the plane normal to the Earth-spacecraft direction. In the figure, the orbit inclination, i , is the angle between the normal to the spacecraft orbit and the Earth-spacecraft direction; the line of nodes is the intersection of the orbit plane and the plane of the sky; the node with respect to the plane of the sky, Ω , is measured in the plane of the sky from a reference direction to the line of nodes; and the argument of periapsis, ω , is the angle between the line of nodes and periapsis measured in the orbit plane.

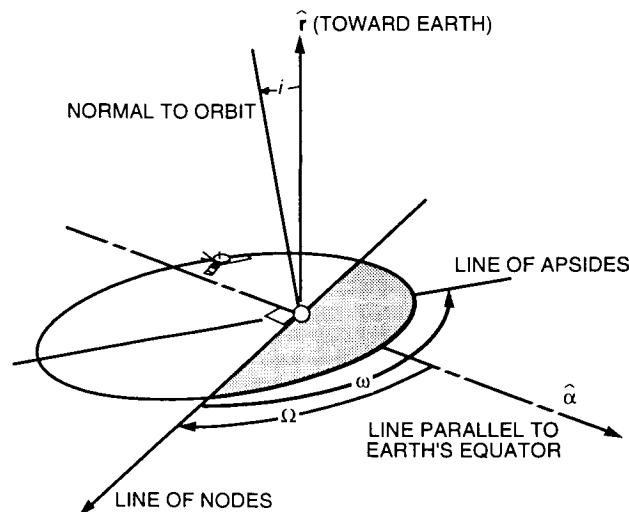


Fig. A-1. Planetary orbiter geometry.

At times, the desired orbit accuracy is greater than what can be achieved with two-way Doppler tracking alone. In the case of Magellan, the desired orbit accuracy was about 1 km for purposes of aligning radar images. This level of accuracy was better than what could be achieved using Doppler data alone. Differential data types such as differenced one-way Doppler (DOD), delta-differenced one-way Doppler (Δ DOD), or two-way minus three-way Doppler (2DM3D) have been shown to improve orbit determination accuracy [26]; the latter was used successfully for Magellan operations [27]. These differential data types are sensitive to Earth orientation errors. An assessment of the characteristic sensitivity to Earth orientation errors for planetary orbiter navigation when using differential data types is described below. The planetary orbiter scenario is based on the radar mapping phase of the Magellan mission.

Consider the geometry drawn schematically in Fig. A-2. The plane of the figure is taken to be the Earth's equatorial plane. (Note that Venus need not lie in the equatorial plane for the analysis to be valid.) Two stations at different complexes are located at the ends of the baseline vector with equatorial projection, b_e . For illustration purposes, an orbit is considered with the orbit plane perpendicular to the Earth's equatorial plane and with the normal to the orbit plane perpendicular to the Earth-Venus direction.

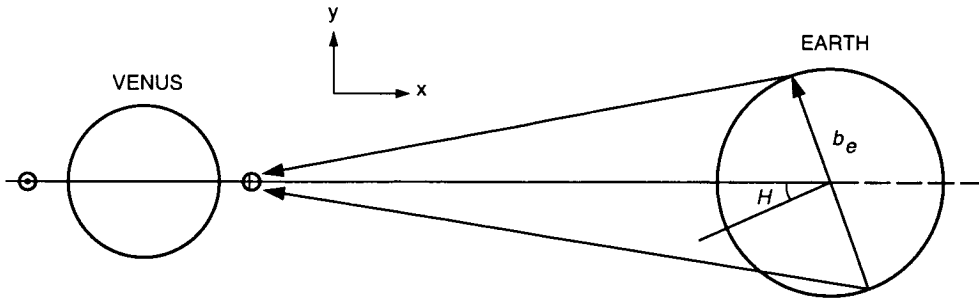


Fig. A-2. Differenced Doppler measurement geometry used in the case study.

DOD measurements are formed by differencing the one-way Doppler signals received by two tracking stations separated by large distances [26]. These measurements give the difference in spacecraft line-of-sight velocity as observed by the two stations. (The 2DM3D measurements exhibit the same information content except for a slight difference resulting from use of a DSN uplink signal rather than the spacecraft onboard oscillator as the reference frequency.) For spacecraft at interplanetary distances, the DOD observable can be approximated as

$$DOD \approx \frac{d}{dt} \left(\mathbf{b} \cdot \frac{\mathbf{r}}{r} \right) \approx \frac{1}{r} \left[\mathbf{b} \cdot \left(\mathbf{v} - \dot{r} \frac{\mathbf{r}}{r} \right) + \left(\frac{\mathbf{r}}{r} \times \boldsymbol{\omega}_e \right) \cdot \mathbf{b} \right] \quad (\text{A-1})$$

where \mathbf{b} is the baseline vector between the two tracking stations, \mathbf{r} is the vector from the center of the Earth to the spacecraft with magnitude r , \dot{r} is the rate of change of distance between the Earth and the spacecraft, \mathbf{v} is the spacecraft velocity vector with magnitude v , and $\boldsymbol{\omega}_e$ is the Earth's rotation rate vector. By considering a DOD measurement for this special case, at the time when the spacecraft velocity is parallel to the Earth's pole, the DOD observable can be further approximated as

$$DOD \approx \frac{1}{r} v_y b_e \cos H + \frac{1}{r} v_z b_z + \omega_e b_e \cos H \quad (\text{A-2})$$

where v_y is the component of the spacecraft velocity in the equatorial plane and perpendicular to the Earth-Venus direction (and nominally zero at the measurement time), b_e is the equatorial baseline length,

v_z is the component of the spacecraft velocity parallel to the Earth's pole, b_z is the length of the projection of the baseline length onto the pole direction, and H is the hour angle between the baseline and the spacecraft. A rotation of the orbit about the Earth-Venus line by an angle $\delta\Omega$ changes v_y from zero to $v\delta\Omega$, which is directly observable in the DOD measurement. If the measurement occurred earlier (or later) in the orbit, where the spacecraft velocity vector was along the spacecraft-Earth direction, there would be no change in spacecraft velocity for a change in the orbit node. In this case, the DOD measurement would not be useful. The importance of performing differenced Doppler measurements at optimum times has been well documented in the literature (see, e.g., [25]).

An error in UT1 introduces a bias in the hour angle, H , and, hence, in the DOD measurement. This can affect the determination of the spacecraft node angle. A change in the measurement due to a calibration error, $\delta UT1$, is approximately given by

$$\delta DOD \approx -b_e \omega_e^2 \sin H \delta UT1 \quad (\text{A-3})$$

This change will cause an error to be inferred in the rotation about the line of sight by an amount

$$\delta\Omega \approx \frac{r}{v} \omega_e^2 \tan H \delta UT1 \quad (\text{A-4})$$

For DSN baselines (Goldstone-Madrid and Goldstone-Canberra), H can vary from about -30 to $+30$ deg, outside of which the spacecraft will fall below the horizon of one of the complexes. DSN baselines have a mean equatorial length of about 8000 km. For the worst case where $H = 30$ deg, a 1-ms error in UT1 will bias the DOD measurements by about 0.02 mm/s. For an orbiter characteristic of Magellan during its mapping phase, with an average orbital velocity, v of about 5.5 km/s, and a line-of-sight distance of 1 AU, a 1-ms timing error in UT1 would lead to a node error of up to 0.08 mrad. With a semimajor axis of 10,000 km, this corresponds to an orbit error of about 0.8 km. (Since this is comparable to the desired orbit accuracy for Magellan, it was necessary to have UT1 calibrated with submillisecond accuracy in order to support the generation of daily orbit determination solutions.)

In general, the maximum sensitivity of the differenced Doppler data to Earth orientation errors is of nearly the same magnitude as for the special case studied here. Sensitivity to Earth orientation errors can be an order of magnitude smaller if the data are acquired at times where the baseline hour angle is near zero and the spacecraft velocity at that time is in a direction where the data are sensitive to the spacecraft node. The size of the orbit errors also depends on (among a number of other factors) the shape of the orbit, the uncertainty in the gravity field, and the amount of Doppler data to be used in the "fit" (i.e., the data filtering process).

Appendix B

Definition of Aiming Plane (*B*-Plane) Coordinates

Planetary approach trajectories are typically described in aiming plane coordinates, often referred to as “*B*-plane” coordinates (see Fig. B-1). This coordinate system was originally conceived to simplify the targeting of a hyperbolic flyby trajectory and is defined by three orthogonal unit vectors, $\hat{\mathbf{S}}$, $\hat{\mathbf{T}}$, and $\hat{\mathbf{R}}$, with the system origin taken to be the gravitational center of mass of the target planet [27]. The $\hat{\mathbf{S}}$ is directed parallel to the incoming spacecraft asymptotic velocity vector relative to the target planet, while $\hat{\mathbf{T}}$ is normally specified to lie in either the ecliptic plane (the mean plane of the Earth’s orbit) or the equatorial plane of the target planet.²⁷ In addition, $\hat{\mathbf{T}}$ is directed perpendicular to $\hat{\mathbf{S}}$. The unit vector $\hat{\mathbf{R}}$ completes an orthogonal triad with $\hat{\mathbf{S}}$ and $\hat{\mathbf{T}}$, thus, $\hat{\mathbf{R}} = \hat{\mathbf{S}} \times \hat{\mathbf{T}}$.

The aim point for a planetary encounter is defined by the impact parameter, \mathbf{B} , which approximates where the point of closest approach would be if the target planet had no mass and did not deflect the flight path. The impact parameter \mathbf{B} is directed perpendicular to $\hat{\mathbf{S}}$; therefore, it lies in the $\hat{\mathbf{T}} - \hat{\mathbf{R}}$ plane. To gain insight into targeting accuracy, orbit determination errors are often characterized by the 1-sigma or 3-sigma uncertainty in the respective “miss components” of \mathbf{B} , namely, $\mathbf{B} \cdot \hat{\mathbf{R}}$ and $\mathbf{B} \cdot \hat{\mathbf{T}}$. These quantities are analogous to elevation and azimuth when specifying the impact point for terrestrial targets.

The time from encounter is defined by the linearized time of flight (LTOF), a quantity which is a measure of the “time-to-go” from the current spacecraft position to the intersection of its asymptotic flight path and the aiming plane. LTOF provides a convenient time-to-go parameter because LTOF is not affected by changes in the $\mathbf{B} \cdot \hat{\mathbf{R}}$ and $\mathbf{B} \cdot \hat{\mathbf{T}}$ miss components.²⁸ Orbit determination errors are also characterized by the 1-sigma or 3-sigma uncertainty in LTOF.

In lieu of using $\mathbf{B} \cdot \hat{\mathbf{R}}$ and $\mathbf{B} \cdot \hat{\mathbf{T}}$ uncertainties to measure targeting accuracy, a 1-sigma or 3-sigma *B*-plane dispersion ellipse (also shown in Fig. B-1) is often used. The semimajor (SMAA) and semiminor (SMIA) axes of the dispersion ellipse are related in quadrature to the uncertainties of $\mathbf{B} \cdot \hat{\mathbf{R}}$ and $\mathbf{B} \cdot \hat{\mathbf{T}}$. The angle θ_T gives the angle clockwise from $\hat{\mathbf{T}}$ to the SMAA.

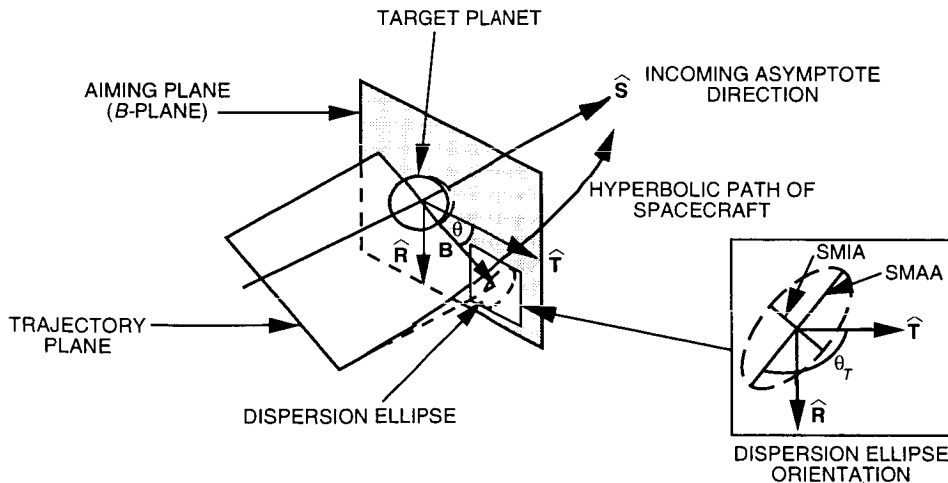


Fig. B-1. The aiming plane (*B*-plane) coordinate system.

²⁷ For the analysis presented in this article, $\hat{\mathbf{T}}$ was specified to lie in the Earth’s equatorial plane.

²⁸ R. A. Jacobson, “Linearized-Time-of-Flight Revisited,” JPL Engineering Memorandum 391-680 (Revised) (internal document), Jet Propulsion Laboratory, Pasadena, California, September 22, 1975.